OPTIMIZED SCHWARZ WAVEFORM RELAXATION METHODS FOR THE TELEGRAPHER EQUATION*

MOHAMMAD D. AL-KHALEEL†, MARTIN J. GANDER‡, AND PRATIK M. KUMBHAR§

Abstract. Schwarz waveform relaxation (SWR) methods are popular domain decomposition methods for solving time dependent problems. Optimized SWR algorithms (OSWR) are a modern class of SWR algorithms using transmission conditions that exchange more information and involve parameters that can be used to optimize the convergence rate of OSWR. We present here an analysis of overlapping and nonoverlapping SWR and OSWR applied to the telegrapher equation. We derive explicit asymptotic expressions for the optimized parameters, and show their great impact on the convergence of OSWR. We also explain how closely the telegrapher equation is related to RLCG transmission line circuits, and construct new discretization schemes based on this relation, with stability and convergence analyses. We illustrate our theoretical results with numerical experiments.

AMS subject classifications. 65M55, 65M06, 65L10

Key words. Domain decomposition methods; Schwarz waveform relaxation methods; optimized transmission conditions; telegrapher equation; RLCG electric circuits.

1. Introduction.

Transmission lines are structures designed to transport electricity or electric signals from one place to another with minimum loss and distortion. Typically, they serve purposes such as distributing cable television signals, transmission of electrical power from generating substations to various distribution units, connecting radio transmitters and receivers, and so on. The so-called telegrapher equation describes the signal propagation in these transmission lines. We consider here the one-dimensional telegrapher equation

$$\mathcal{L}u := \frac{\partial^2 u}{\partial t^2} + (\alpha+\beta)\frac{\partial u}{\partial t} + \alpha\beta u - c_{\text{T}}^2\frac{\partial^2 u}{\partial x^2} = f, \quad (x,t) \in \Omega \times [0,T], \tag{1.1a}$$

with initial conditions

$$u(x,0) = u_0(x), \quad \frac{\partial u}{\partial t}(x,0) = v_0(x), \tag{1.1b}$$

where the domain $\Omega := \mathbb{R}$, $T > 0$ is the final time, the constants $\alpha, \beta > 0$, and c_{T} is the wave speed. The unknown $u(x,t)$ in the telegrapher equation (1.1) is either a current or voltage. The right hand side source term f and initial conditions u_0, v_0 are known continuous real-valued functions, and we assume that solutions remain bounded at infinity. For $\alpha, \beta = 0$, the telegrapher equation (1.1a) reduces to a wave equation, while for large values of $\alpha, \beta, c_{\text{T}} \to \infty$, the limit is a heat type equation. Some analysis in this article concerns the first, wave equation limit.

There are many numerical methods for solving the telegrapher equation, for example finite difference schemes [17, 23, 24], the alternating group explicit method [8], and also collocation methods and spline radial basis functions [7]. However, using domain decomposition (DD) methods for the telegrapher equation to increase the

*version August 16, 2024.

Funding: Funded by the Deutsche Forschungsgemeinschaft (DFG, German Research Foundation) -– Project-ID 258734477 — SFB 1173

†Khalifa University, Abu Dhabi, UAE, and also with Yarmouk University, Irbid, Jordan, (mohammad.alkhaleel@ku.ac.ae).

‡Université de Genève, Genève, Switzerland, (martin.gander@unige.ch).

§Karlsruhe Institute of Technology, Karlsruhe, Germany, (pratik.kumbhar123@gmail.com).

computational efficiency and parallelism is new. The main idea of DD methods is to decompose the domain into subdomains, and solve the problem on these decomposed subdomains instead of solving on the whole domain, see for instance [11] and references therein.

Schwarz waveform relaxation (SWR) methods are popular domain decomposition methods to solve time dependent partial differential equations (PDEs). SWR methods coupled with "smart" transmission conditions along interfaces which contain parameters that can be optimized are called optimized SWR (OSWR). They have been intensively analyzed for wave-type equations, see, e.g., [5, 12], and different parabolic problems, see, e.g., [11, 4]. To further reduce the computational cost, the iterates in these methods can be computed in a parallel pipelined fashion [26, 21].

Another group of domain decomposition methods to treat time-dependent problems consists of Dirichlet-Neumann and Neumann-Neumann waveform relaxation methods [22, 25, 20]. These are nonoverlapping spatial decomposition methods where subdomains are solved with corresponding boundary conditions, followed by a correction step. Recently, they have been coupled with parareal algorithms [29], and pipelined implementations [27].

The telegrapher equations can also be obtained from the mathematical modeling of RLCG transmission lines, where $\mathrm{R}, \mathrm{L}, \mathrm{C}, \mathrm{G}$ stand for resistance, inductance, capacitance, and conductance respectively. There are extensive analyses of Optimized Waveform Relaxation (OWR) methods applied to RC and RLC circuits; see, e.g., [2, 15, 10]. However, the complete analysis of OWR for complete RLCG circuits is missing. Moreover, the application of WR for field-circuit coupling is gaining importance; see [30, 6, 31] and references therein for more details. In this paper, we present for the first time a combined study of PDEs and circuits. On the one hand, the analysis of OSWR for the telegrapher equation will help to understand field-circuit coupling for more complicated circuits, while on the other hand, the circuit analysis will provide more insight into the choice of approximation of transmission conditions.

In this paper, we propose and analyze both overlapping and nonoverlapping SWR and OSWR methods for the telegrapher equation. Section 2 is dedicated to the derivation of the convergence factors of SWR and OSWR with first-order transmission conditions. In Section 3, we show the relation between the telegrapher equation and the RLCG transmission line, and their convergence factors when applying OWR and OSWR. Section 4 is devoted to the derivation of asymptotic expressions for the optimized parameters. In Section 5, we propose new discretization schemes and analyze their stability and convergence. Finally, we support our theoretical results with numerical experiments in Section 6.

2. Schwarz Waveform Relaxation.

To present and analyze Schwarz Waveform Relaxation (SWR) to solve the telegrapher equation (1.1), we decompose for simplicity the domain Ω into two subdomains, $\Omega = \Omega_1 \cup \Omega_2$ with $\Omega_1 := (-\infty, l]$, $\Omega_2 := [0, \infty)$, with overlap $l \geq 0$ (the extension of SWR to many subdomains is straightforward).

2.1. Classical SWR.

SWR for (1.1) solves for iteration index $k \geq 1$

$$
\begin{aligned}
\mathcal{L}(u_1^k) &= f_{|\Omega_1} \, \mathrm{in} \, \Omega_1 \times (0,T], & \mathcal{L}(u_2^k) &= f_{|\Omega_2} \, \mathrm{in} \, \Omega_2 \times (0,T], \\
u_1^k(l,t) &= u_2^{k-1}(l,t) \, \mathrm{in} \, (0,T], & u_2^k(0,t) &= u_1^{k-1}(0,t) \, \mathrm{in} \, (0,T], \\
u_1^k(x,0) &= u_{0_{|\Omega_1}}(x) \, \mathrm{in} \, \Omega_1, & u_2^k(x,0) &= u_{0_{|\Omega_2}}(x) \, \mathrm{in} \, \Omega_2, \\
\tfrac{\partial}{\partial t} u_1^k(x,0) &= v_{0_{|\Omega_1}}(x) \, \mathrm{in} \, \Omega_1, & \tfrac{\partial}{\partial t} u_2^k(0,0) &= v_{0_{|\Omega_2}}(x) \, \mathrm{in} \, \Omega_2,
\end{aligned}
\tag{2.1}
$$

with arbitrary initial guesses $u_2^0(l,t)$ and $u_1^0(0,t)$. To study the convergence of SWR, we use the error equations in Laplace space: let $\mathrm{e}_j^k(x,t) := u_j^k(x,t) - u_{|\Omega_j}(x,t)$ be the error between the subdomain solution u_j^k at iteration k and the exact solution restricted to subdomain Ω_j, $j \in \{1,2\}$. Taking a Laplace transform of the error equations of (2.1) on Ω_1, i.e. the equations with zero data, yields $s^2\hat{\mathrm{e}}_1^k + (\alpha+\beta)s\hat{\mathrm{e}}_1^k + \alpha\beta\hat{\mathrm{e}}_1^k = c_{\mathrm{T}}^2\frac{\partial^2\hat{\mathrm{e}}_1^k}{\partial x^2}$ for $s \in \mathbb{C}$. Solving this equation using its characteristic equation leads to $\hat{\mathrm{e}}_1^k(x) = A_1^k e^{\lambda x} + B_1^k e^{-\lambda x}$, where $\lambda(s) := \sqrt{\frac{(s+\alpha)(s+\beta)}{c_{\mathrm{T}}^2}}$. To simplify the notation, we drop the dependence of λ on s, $\lambda = \lambda(s)$ and only explicitly mention it when needed. Similarly, the error in Ω_2 can be expressed as $\hat{\mathrm{e}}_2^k(x) = A_2^k e^{\lambda x} + B_2^k e^{-\lambda x}$. Since the errors like the solutions need to remain bounded when $x \to \pm\infty$, we must have

$$\hat{\mathrm{e}}_1^k(x) = A_1^k e^{\lambda x}, \quad \text{and} \quad \hat{\mathrm{e}}_2^k(x) = B_2^k e^{-\lambda x}, \tag{2.2}$$

where the constants A_1^k and B_2^k at the k^{th} iterate are determined using the transmission conditions. For classical SWR, the transmission conditions from (2.1) are

$$\hat{\mathrm{e}}_1^{k+1}(l) = \hat{\mathrm{e}}_2^k(l), \quad \text{and} \quad \hat{\mathrm{e}}_2^{k+1}(0) = \hat{\mathrm{e}}_1^k(0). \tag{2.3}$$

Substituting the expressions of $\hat{\mathrm{e}}_1^k$ and $\hat{\mathrm{e}}_2^k$ given in (2.2) into (2.3) leads to $A_1^{k+1} = e^{-2\lambda l}B_2^k$ and $B_2^{k+1} = A_1^k$, which results in $\hat{\mathrm{e}}_1^{k+1}(x) = \rho_{\mathrm{SWR}}(s,l)\hat{\mathrm{e}}_1^{k-1}(x)$ and $\hat{\mathrm{e}}_2^{k+1}(x) = \rho_{\mathrm{SWR}}(s,l)\hat{\mathrm{e}}_2^{k-1}(x)$, with the convergence factor of classical SWR given by

$$\rho_{\mathrm{SWR}}(s,l) := e^{-2\lambda l}, \quad \text{with} \quad \lambda(s) = \sqrt{\frac{(s+\alpha)(s+\beta)}{c_{\mathrm{T}}^2}}. \tag{2.4}$$

We see from (2.4) that for overlap $l = 0$, $|\rho_{\mathrm{SWR}}(s,0)| = 1$ and hence SWR does not converge. For $l > 0$, the convergence factor satisfies $|\rho_{\mathrm{SWR}}(s,l)| < 1$ for all $s \in \mathbb{C}$ with $\Re(s) > 0$. Overlap is thus necessary for SWR to converge, and the convergence rate can be increased by increasing the overlap.

2.2. Optimized SWR. To improve convergence, we introduce in (2.1) the more general transmission conditions

$$\left(\tfrac{\partial}{\partial x} + \mathcal{S}_1\right)u_1^{k+1}(l) = \left(\tfrac{\partial}{\partial x} + \mathcal{S}_1\right)u_2^k(l),\ \left(\tfrac{\partial}{\partial x} + \mathcal{S}_2\right)u_2^{k+1}(0) = \left(\tfrac{\partial}{\partial x} + \mathcal{S}_2\right)u_1^k(0), \tag{2.5}$$

where the operators $\mathcal{S}_j, j = 1,2$ are acting along the interface. For example, if $\mathcal{S}_j$ is constant, say $\mathcal{S}_j \equiv \sigma \in \mathbb{R}$ and σ is large, then we are back to classical transmission conditions. We call the SWR algorithm with such transmission conditions Optimized SWR (OSWR), since the operators $\mathcal{S}_j$ can be optimized to achieve rapid convergence.

We now derive an explicit expression of the convergence factor of OSWR, by substituting the analytic expressions of the errors in (2.2) into the new transmission conditions (2.5), yielding $(\lambda+\sigma_1)A_1^{k+1}e^{\lambda l} = (-\lambda+\sigma_1)B_2^k e^{-\lambda l}$ and $(-\lambda+\sigma_2)B_2^{k+1} = (\lambda+\sigma_2)A_1^k$, where σ_j denotes the symbol for the Laplace transform of the operators $\mathcal{S}_j$. These coupled equations simplify to

$$A_1^{k+1} = \frac{(\sigma_1-\lambda)(\sigma_2+\lambda)}{(\sigma_1+\lambda)(\sigma_2-\lambda)}e^{-2\lambda l}A_1^{k-1}, \quad \text{and} \quad B_2^{k+1} = \frac{(\sigma_1-\lambda)(\sigma_2+\lambda)}{(\sigma_1+\lambda)(\sigma_2-\lambda)}e^{-2\lambda l}B_2^{k-1}.$$

Iterating these relations $2k$ times yields $\hat{\mathrm{e}}_1^{2k}(x) = \rho_{\mathrm{opt}}(s,l,\sigma_1,\sigma_2)^k\hat{\mathrm{e}}_1^0(x)$ and $\hat{\mathrm{e}}_2^{2k}(x) = \rho_{\mathrm{opt}}(s,l,\sigma_1,\sigma_2)^k\hat{\mathrm{e}}_2^0(x)$, where the convergence factor ρ_{opt} is given by

$$\rho_{\mathrm{opt}}(s,l,\sigma_1,\sigma_2) := \frac{(\sigma_1-\lambda)(\sigma_2+\lambda)}{(\sigma_1+\lambda)(\sigma_2-\lambda)}e^{-2\lambda l}, \quad \lambda(s) = \sqrt{\frac{(s+\alpha)(s+\beta)}{c_{\mathrm{T}}^2}}. \tag{2.6}$$

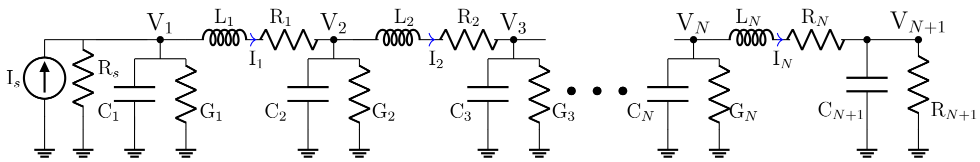

Fig. 3.1: A lumped RLCG transmission line model with N nodes.

For rapid convergence, we would like to have the modulus of the convergence factor as small as possible. In fact, by choosing

$$\sigma_1 := \lambda, \quad \text{and} \quad \sigma_2 := -\lambda, \tag{2.7}$$

the convergence factor (2.6) vanishes identically, $\rho(s, l, \lambda, -\lambda) \equiv 0$, and OSWR then converges in two iterations independently of overlap l, and we have a direct solver. However, the inverse Laplace transform of λ leads to non-local operators in time since λ contains square root terms (see [9] for more details). One thus needs to use in practice an approximation of these symbols $\sigma_j, j = 1, 2$. Moreover, the optimal parameters given by equation (2.7) suggest that one can assume $\sigma_1 = \sigma$ and $\sigma_2 = -\sigma$, and thus the convergence factor (2.6) reduces to

$$\rho_{\text{opt}}(s, l, \sigma) := \left(\frac{\sigma - \lambda}{\sigma + \lambda}\right)^2 e^{-2\lambda l}. \tag{2.8}$$

This shows that the effect of overlap given by the term $e^{-2\lambda l}$ is the same as for classical SWR. The difference lies in a smart choice of σ, which we will determine in Section 4. Before, we however present now a discrete model for transmission lines given by an electric circuit, and their WR algorithms and convergence factors.

3. Circuits.

In this section, we derive a mathematical model of RLCG circuits, apply WR and OWR algorithms to it, deduce their convergence factors, and show their relation to the convergence factor of the telegrapher equation. The relation between the telegrapher equation and circuits will then help in developing and analyzing fully discrete schemes for the telegrapher equation, which are discussed in Section 5.

As discussed in Section 1, transmission lines can also be modeled by circuits, which are discrete models, represented by circuit elements, and it is the RLCG TL model circuit shown in Fig. 3.1 that models a transmission line [1]. Assuming that the lumped RLCG TL model circuit has N nodes and that the circuit is infinitely long, an application of the modified nodal analysis (MNA) method [18] to the circuit model in Fig. 3.1 yields the system of ODEs

$$\frac{d\mathbf{w}}{dt} = \begin{pmatrix} \ddots & \ddots & \ddots & & & & & \\ & a & b & -a & & & & \\ & & -c & \tilde{b} & c & & & \\ & & & a & b & -a & & \\ & & & & -c & \tilde{b} & c & \\ & & & & & \ddots & \ddots & \ddots \end{pmatrix} \mathbf{w} + \mathbf{f}, \tag{3.1}$$

where the solution vector $\mathbf{w} = (\dots, w_{-1}, w_0, w_1, \dots)^\top$ is ordered such that nodal voltages alternate with currents between them. The odd index rows with c and $\tilde{b}$ elements correspond to voltage unknowns, and the even index rows with a and b elements correspond to current unknowns. The constant entries of the matrix are given by $a = \frac{1}{\mathrm{L}_i} > 0$, $b = -\frac{\mathrm{R}_i}{\mathrm{L}_i} \leq 0$, $\tilde{b} = -\frac{\mathrm{G}_i}{\mathrm{C}_i} \leq 0$ and $c = -\frac{1}{\mathrm{C}_i} < 0$, where the characteristic electronic component parameters are $\mathrm{R}_i = \frac{\mathrm{R}}{N}$, $\mathrm{L}_i = \frac{\mathrm{L}}{N}$, $\mathrm{C}_i = \frac{\mathrm{C}}{N}$, and $\mathrm{G}_i = \frac{\mathrm{G}}{N}$. The source term on the right hand side is given by the vector of functions $\mathbf{f}(t) = (\dots, f_{-1}(t), f_0(t), f_1(t), \dots)^\top$, and an initial condition $\mathbf{w}^0 = (\dots, w^0_{-1}, w^0_0, w^0_1, \dots)^\top$ is needed. Since the circuit is infinitely large, we need to assume that all unknowns are bounded as we move toward the ends of the circuit to have a well posed problem.

Defining $\bar{a} = \frac{a}{N} = \frac{1}{\mathrm{L}}$, and $\bar{c} = \frac{c}{N} = -\frac{1}{\mathrm{C}}$ with space discretization parameter $h \approx \frac{1}{N} \to 0$, the system of ODEs (3.1) for $\mathbf{f} \equiv 0$ can be considered as a discretization of

$$\frac{\partial \mathrm{I}}{\partial t} = -\bar{a}\frac{\partial \mathrm{V}}{\partial x} + b\mathrm{I}, \quad \text{and} \quad \frac{\partial \mathrm{V}}{\partial t} = \bar{c}\frac{\partial \mathrm{I}}{\partial x} + \tilde{b}\mathrm{V}. \tag{3.2}$$

One can easily see this by using forward and backward finite differences with space step h for the first and second equations in (3.2), respectively. Further combining these two first-order coupled equations leads to a second-order telegrapher equation (1.1a) of the form

$$\mathrm{LC}\frac{\partial^2 \mathrm{w}}{\partial t^2} + (\mathrm{RC} + \mathrm{GL})\frac{\partial \mathrm{w}}{\partial t} + \mathrm{GR}\mathrm{w} = \frac{\partial^2 \mathrm{w}}{\partial x^2}, \tag{3.3}$$

where the unknown w is either a voltage (V) or a current (I). Comparing equation (3.3) with (1.1a), we see that $\bar{a}|\bar{c}| = c_{\mathrm{T}}^2 = \frac{1}{\mathrm{LC}} > 0$, $|b| = \alpha = \frac{\mathrm{R}}{\mathrm{L}} \geq 0$ and $|\tilde{b}| = \beta = \frac{\mathrm{G}}{\mathrm{C}} \geq 0$.

3.1. Comparison of the optimizing parameters. The ultimate aim of this subsection is to show the relation between the convergence factor (2.8) of the telegrapher equation (1.1a) and that of the RLCG circuit from Fig. 3.1, which represents a semi-discretization of the telegrapher equation (3.2), and hence obtain the relation between the corresponding optimizing parameters.

Partitioning the circuit system (3.1) at an odd index row, i.e., at a row corresponding to a voltage unknown, into two subcircuits (subsystems) with overlap ensuring that both types of variables are covered, and using a Laplace transform with parameter $s = \eta + i\omega \in \mathbb{C}$, the convergence factor for the optimized WR algorithm was given in [1], and can be written including h as

$$\rho_{\mathrm{opt}}^{\mathrm{RLCG}}(s, \gamma_1, \gamma_2) = \begin{cases} \dfrac{(s-\tilde{b})\mu_- + \gamma_1 \frac{|\bar{c}|}{h}(\mu_- - 1)}{(s-\tilde{b}) + \gamma_1 \frac{|\bar{c}|}{h}(1-\mu_-)} \cdot \dfrac{\frac{|\bar{c}|}{h}(1-\mu_-) + \gamma_2(s-\tilde{b})\mu_-}{\frac{|\bar{c}|}{h}(\mu_- - 1) + \gamma_2(s-\tilde{b})}, & |\mu_+| > 1, \\ \dfrac{(s-\tilde{b})\mu_+ + \gamma_1 \frac{|\bar{c}|}{h}(\mu_+ - 1)}{(s-\tilde{b}) + \gamma_1 \frac{|\bar{c}|}{h}(1-\mu_+)} \cdot \dfrac{\frac{|\bar{c}|}{h}(1-\mu_+) + \gamma_2(s-\tilde{b})\mu_+}{\frac{|\bar{c}|}{h}(\mu_+ - 1) + \gamma_2(s-\tilde{b})}, & |\mu_+| < 1, \end{cases} \tag{3.4}$$

where γ_1, γ_2 are the optimizing parameters, and

$$\mu_\pm = \frac{\frac{2\bar{a}|\bar{c}|}{h^2} + (|\tilde{b}| + s)(|b| + s) \pm \sqrt{\left(\frac{2\bar{a}|\bar{c}|}{h^2} + (|\tilde{b}| + s)(|b| + s)\right)^2 - \frac{4\bar{a}^2|\bar{c}|^2}{h^4}}}{\frac{2\bar{a}|\bar{c}|}{h^2}}. \tag{3.5}$$

We assume $\gamma_1 = -\frac{1}{\gamma_2}$, which is motivated by the optimal choice in [1], as we did for the telegrapher equation, and we let $\gamma_2 := \gamma$. Then using the relations $\mu_+\mu_- = 1$,

$\bar{c} = -|\bar{c}|$, and $\tilde{b} = -|\tilde{b}|$, the convergence factor in (3.4) reduces to

$$\rho_{\text{opt}}^{\text{RLCG}}(s,\gamma) = \begin{cases} \left(\frac{\gamma(s+|\tilde{b}|)+\frac{|\bar{c}|}{h}(1-\mu_+)}{\gamma(s+|\tilde{b}|)+\frac{|\bar{c}|}{h}(1-\mu_-)} \cdot \mu_- \right)^2, & |\mu_+| > 1, \\ \left(\frac{\gamma(s+|\tilde{b}|)+\frac{|\bar{c}|}{h}(1-\mu_-)}{\gamma(s+|\tilde{b}|)+\frac{|\bar{c}|}{h}(1-\mu_+)} \cdot \mu_+ \right)^2, & |\mu_+| < 1. \end{cases} \tag{3.6}$$

We can now link the transmission conditions in the RLCG circuit case [1] with the ones we proposed for the telegrapher equation, to see how σ in (2.8) is related to γ from the circuit case in (3.6). For this, we first show that as $h \to 0$, the convergence factor of OWR from the circuit in (3.6) converges to the convergence factor of the OSWR for the telegrapher equation in (2.8).

We consider the case when $|\mu_+| > 1$, the case $|\mu_+| < 1$ can be shown similarly. Note that λ in (2.6) can be written in terms of the RLCG circuit elements and parameters as $\lambda = \sqrt{\frac{(s+|b|)(s+|\tilde{b}|)}{\bar{a}|\bar{c}|}}$. Note that in [1] only OWR with minimum overlap was considered, i.e., $l = h$. A Taylor expansion of $\mu_\pm$ in (3.5) for small h leads to $\mu_- = e^{-\lambda h} + \mathcal{O}(h^2)$ and $\mu_+ = e^{\lambda h} + \mathcal{O}(h^2)$, or equivalently $\frac{1-\mu_-}{h} = \lambda + \mathcal{O}(h)$ and $\frac{1-\mu_+}{h} = -\lambda + \mathcal{O}(h)$. Therefore, as $h \to 0$, the effect of overlap μ_-^2 in (3.6) for circuits converges to that of $e^{-2\lambda h}$ in (2.8) of the telegrapher equation. For larger overlap $l > h$, one can use a similar analysis and compare the convergence factor of overlapping OWR applied to infinitely long RLCG circuits found in [19, Chapter 3].

Finally we evaluate the limit of the remaining term in $\rho_{\text{opt}}^{\text{RLCG}}$,

$$\lim_{h\to 0} \left(\frac{\gamma(s+|\tilde{b}|)+\frac{|\bar{c}|}{h}(1-\mu_+)}{\gamma(s+|\tilde{b}|)+\frac{|\bar{c}|}{h}(1-\mu_-)} \right) = \frac{\gamma(s+|\tilde{b}|)-|\bar{c}|\lambda}{\gamma(s+|\tilde{b}|)+|\bar{c}|\lambda} = \frac{\frac{\gamma}{|\bar{c}|}s + \frac{\gamma|\tilde{b}|}{|\bar{c}|} - \lambda}{\frac{\gamma}{|\bar{c}|}s + \frac{\gamma|\tilde{b}|}{|\bar{c}|} + \lambda}.$$

Considering a first-order approximation of σ in (2.8), that is $\sigma = p + qs$, and by combining the above results, we obtain that $\rho_{\text{opt}}^{\text{RLCG}} \to \rho_{\text{opt}}$ as $h \to 0$ with

$$p = \frac{\gamma|\tilde{b}|}{|\bar{c}|}, \quad \text{and} \quad q = \frac{\gamma}{|\bar{c}|}. \tag{3.7}$$

We can thus obtain optimized parameters for first-order approximations of the transmission conditions for the telegrapher equation with constants $p > 0$ and $q > 0$ using $\gamma > 0$ from the RLCG circuit [1]. However, it has to be noted that γ was optimized only numerically in [1] for the complete RLCG circuit case, and certain analytical expressions for optimized γ are available only when OWR is applied to the simpler RLC and LCG circuits from [19, 10, 14], but not for the complete RLCG circuit. Additionally, when using (3.7), both parameters p and q are obtained via optimization of only one parameter γ. Therefore, a more thorough analysis of OSWR for the telegrapher equation is needed, in order to get a full understanding of how to optimize parameters, also in the case of RLCG circuits.

4. Optimization.

In this section, we optimize the convergence factor ρ_{opt} (2.8) of the telegrapher equation by making its modulus as small as possible using σ. This leads to the min-max problem

$$\min_{\sigma} \max_{s\in\mathbb{C}} |\rho_{\text{opt}}(s,l,\sigma)|, \quad \text{where} \quad \rho_{\text{opt}}(s,l,\sigma) = \left(\left(\frac{\sigma-\lambda}{\sigma+\lambda} \right) e^{-\lambda l} \right)^2. \tag{4.1}$$

We use for σ a polynomial in s. To simplify the min-max problem (4.1), we need

LEMMA 4.1. *If $\alpha \geq 0$, $\beta \geq 0$ and $\Re(\sigma) \geq 0$ then the convergence factor ρ_{opt} in* (2.8) *is an analytic function in the right half of the complex plane.*

Proof. λ is an analytic function in the right half of the complex plane since $\Im((s+\alpha)(s+\beta)) = 0$ only when $\omega = 0$ but for $\omega = 0$, we have $\Re((s+\alpha)(s+\beta)) > 0$ and hence the argument under the square root avoids the negative real axis. Moreover, for $\Re(\sigma) \geq 0$ and since $\Re(\lambda(s)) > 0$ in the right half of the complex plane, the denominator $\sigma + \lambda$ does not vanish. Hence, the convergence factor ρ_{opt} is an analytic function in the right half of the complex plane. ∎

Using the maximum principle of analytic functions, the maximum of $|\rho_{\text{opt}}(s, l, \sigma)|$ lies on the imaginary axis, that is, on $s = i\omega$. Furthermore using complex analysis techniques similar to the ones used in [15, Lemma 4], one can show that for $s = i\omega$, $\omega \in \mathbb{R}$, the modulus of the convergence factor (2.8) satisfies the relation $|\rho_{\text{opt}}(i\omega, l, \sigma)| = |\rho_{\text{opt}}(-i\omega, l, \sigma)|$, which further restricts the range of ω in $s = i\omega$ from $\omega \in \mathbb{R}$ to $\omega \geq 0$.

We now look at the optimization parameter σ. Motivated by the relation with RLCG circuits and their convergence factor in Section 3, we consider first-order approximations of σ, that is, we replace σ by $p + qi\omega$, where $p, q \in \mathbb{R}$, with $p, q > 0$ and i is the imaginary unit. This choice is motivated by the study of OSWR for one-dimensional wave equations in [13], where time derivatives were essential in the transmission conditions to achieve good convergence.

Our main goal is to solve the min-max problem

$$\min_{p,q\in\mathbb{R}} \left(\max_{\omega\geq 0} |\rho_{\text{opt}}(\omega, l, p, q)|\right), \ \rho_{\text{opt}}(\omega, l, p, q) = \left(\frac{p+iq\omega-\lambda}{p+iq\omega+\lambda} e^{-\lambda l}\right)^2, \tag{4.2}$$

with $\lambda = \sqrt{\frac{(i\omega+\alpha)(i\omega+\beta)}{c_{\text{T}}^2}}$. Since $|\rho_{\text{opt}}(\omega, l, p, q)|$ is a complicated function of ω, p and q, deriving an analytic solution of (4.2) is not possible. We therefore use asymptotics to solve the min-max problem (4.2). We observe that $\alpha = \frac{\text{R}}{\text{L}}$ and $\beta = \frac{\text{G}}{\text{C}}$, where the resistance R is much larger than the conductance G, and thus we have $\beta \ll \alpha$. This motivates us to assume that $\beta = \epsilon\alpha$, where $\epsilon > 0$ is a small parameter. Note that one can also use the same analysis when $\alpha \ll \beta$, with $\beta = \frac{1}{\epsilon}\alpha$, because the telegrapher equation (1.1a) remains the same when one interchanges α and β. A special case is $\alpha = \beta$: the convergence parameter $\lambda(\omega)$ then simplifies to $\lambda(\omega) = \frac{i\omega+\alpha}{c_T}$, and choosing $p = \frac{\alpha}{c_T}$, $q = \frac{1}{c_T}$ makes the convergence factor $\rho_{\text{opt}}(\omega, l, \frac{\alpha}{c_T}, \frac{1}{c_T}) \equiv 0$. This leads to optimal convergence of OSWR in two iterations.

4.1. The case without overlap. We start with the nonoverlapping case, $l = 0$. Under the assumption $\beta = \epsilon\alpha$, we observe numerically that the solution of the min-max problem (4.2) is given by equioscillation between $\omega = 0$, $\omega = \overline{\omega}$ and $\omega_{\max}$, where $\omega_{\max} \to \infty$ and $0 < \overline{\omega} < \infty$, that is, the convergence factor $\rho_{\text{opt}}(\omega, 0, p, q)$ at optimized parameters p_0^* and q_0^* satisfies the two relations

$$|\rho_{\text{opt}}(0, 0, p_0^*, q_0^*)| = |\rho_{\text{opt}}(\overline{\omega}, 0, p_0^*, q_0^*)| = \lim_{\omega_{\max}\to\infty} |\rho_{\text{opt}}(\omega_{\max}, 0, p_0^*, q_0^*)|, \tag{4.3a}$$

and in addition for the derivative

$$\frac{\partial}{\partial\omega} |\rho_{\text{opt}}(\overline{\omega}, 0, p_0^*, q_0^*)| = 0. \tag{4.3b}$$

Since the frequency $\omega \in [0, \omega_{\max}]$, and $\Re(\lambda) > 0$, from [3] we know that the solution of the min-max problem (4.1) exists, is unique, and is given by equioscillation. To start our analysis, we use Taylor expansions of $\lambda(\omega)$ at the end points $\omega = 0$ and

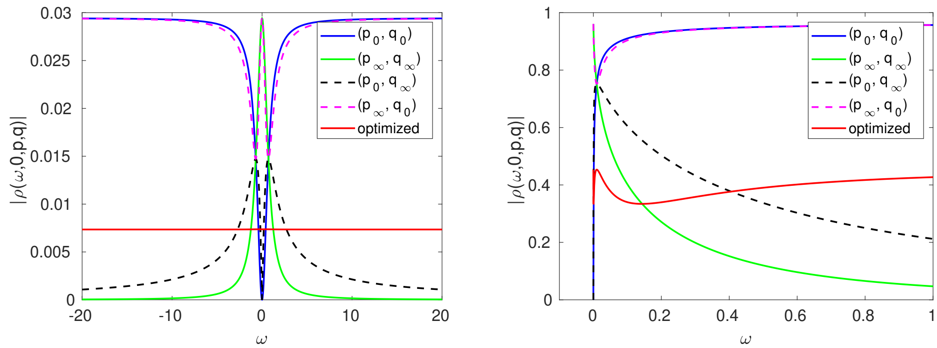

Fig. 4.1: Convergence factor for different values of p and q for $\alpha = 1$, with large $\beta = 0.5$ (left) and with small $\beta = 10^{-4}$ (right).

$\omega_{\max} \to \infty$ to investigate low and high frequency approximations. At $\omega = 0$, we get $\lim_{\omega\to 0} \lambda(\omega) = \frac{\sqrt{\alpha\beta}}{c_{\scriptscriptstyle T}} + \frac{(\alpha+\beta)\omega i}{2c_{\scriptscriptstyle T}\sqrt{\alpha\beta}} + \mathcal{O}(\omega^2)$, yielding the low frequency approximation

$$p_0 := \frac{\sqrt{\alpha\beta}}{c_{\scriptscriptstyle T}}, \quad \text{and} \quad q_0 := \frac{(\alpha+\beta)}{2c_{\scriptscriptstyle T}\sqrt{\alpha\beta}}. \tag{4.4}$$

For $\omega \to \infty$, we get $\lim_{\omega\to\infty} \lambda(\omega) = \frac{\alpha+\beta}{2c_{\scriptscriptstyle T}} + \frac{\omega i}{c_{\scriptscriptstyle T}} + \mathcal{O}(\frac{1}{\omega})$, giving the high frequency approximation

$$p_\infty := \frac{\alpha+\beta}{2c_{\scriptscriptstyle T}}, \quad \text{and} \quad q_\infty = \frac{1}{c_{\scriptscriptstyle T}}. \tag{4.5}$$

In Fig. 4.1, we plot the modulus of the convergence factor $|\rho_{\text{opt}}(\omega, 0, p, q)|$ for different choices of p and q for two different values of $\beta = \alpha\epsilon$. The left plot shows that we achieve rapid convergence with convergence factor modulus around 0.03 when using $p = p_0, p_\infty$ and/or $q = q_0, q_\infty$. However optimization leads to an even better convergence factor of about 0.007. From the right plot of Fig. 4.1, we see that for a small value of ϵ, i.e., β small, the maximum of the convergence factor with $p = p_0, p_\infty$ and $q = q_0, q_\infty$ is close to 1 for small or large ω, and hence the choices of p and q given in (4.4)-(4.5) do not seem good enough. Optimization increases the rate of convergence dramatically, and deriving explicit expressions for optimized parameters $p_{\scriptscriptstyle 0}^*$ and $q_{\scriptscriptstyle 0}^*$ is very much worthwhile.

Further, we observe from the right plot of Fig. 4.1 and left plot of Fig. 4.2, that the solution of the optimization problem (4.2) is given by equioscillation at three points for β small. Also, from the right plot of Fig. 4.2 and the plots of Fig. 4.3, we observe numerically that $p_{\scriptscriptstyle 0}^*, q_{\scriptscriptstyle 0}^*, \overline{\omega} > 0$ with $p_{\scriptscriptstyle 0}^*, \overline{\omega} \to 0$, while $q_{\scriptscriptstyle 0}^* \to \infty$ as $\epsilon \to 0$. We therefore assume $p_{\scriptscriptstyle 0}^* = C_p\epsilon^{\delta_p}$, $\overline{\omega} = C_\omega\epsilon^{\delta_\omega}$, and $q_{\scriptscriptstyle 0}^* = C_q\epsilon^{-\delta_q}$, where the constants $\delta_p, \delta_q, \delta_\omega > 0$. We also observe from the left plot of Fig. 4.3 that C_q does not depend on α, which has been shown analytically in equation (4.12). Further, from the right plot of Fig. 4.2 and the plots of Fig. 4.3, we observe that the values of δ_p, δ_q, and δ_ω are numerically given by $\frac{3}{8}$, $\frac{1}{8}$, and $\frac{1}{2}$, respectively. These values we will determine by analysis in what follows using the equioscillation equations (4.3).

We first find an expression for $|\rho_{\text{opt}}(\omega, 0, p_{\scriptscriptstyle 0}^*, q_{\scriptscriptstyle 0}^*)|$ by substituting the expression of

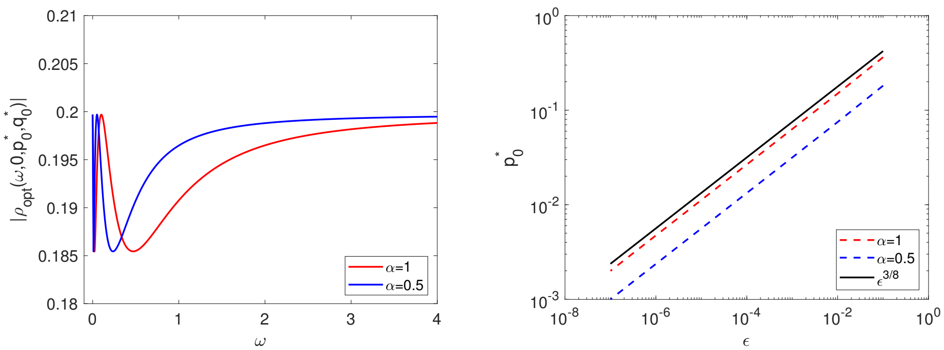

Fig. 4.2: Modulus of the convergence factor at the solution of minmax problem for nonoverlapping case ($l = 0$) (left) and dependence of solution $p_{_0}^*$ on ϵ (right) for different values of α.

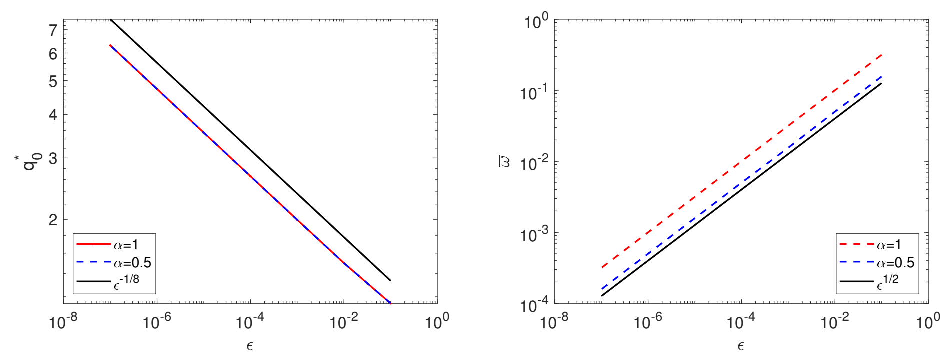

Fig. 4.3: Dependence of solution $q_{_0}^*$ (left) and $\overline{\omega}$ (right) on ϵ for different values of α.

λ. Let $R(\omega, l, p, q) := |\rho_{\text{opt}}(\omega, l, p, q)|$. Then,

$$R(\omega, 0, p_{_0}^*, q_{_0}^*) := |\rho_{\text{opt}}(\omega, 0, p_{_0}^*, q_{_0}^*)| = \frac{r_0 + r_1 - r_2 - r_3 + r_4}{r_0 + r_1 + r_2 + r_3 + r_4}, \tag{4.6a}$$

where

$$r_0 = C_q^2 c_{\text{T}}^2 \omega^2 \epsilon^{-2\delta_q}, \tag{4.6b}$$

$$r_1 = C_p^2 c_{\text{T}}^2 \epsilon^{2\delta_p}, \tag{4.6c}$$

$$r_2 = \left(2\sqrt{(\alpha^2+\omega^2)\left(\omega^2+\alpha^2\epsilon^2\right)} - 2\alpha^2\epsilon + 2\omega^2\right)^{\frac{1}{2}} c_{\tau} C_q \omega \epsilon^{-\delta_q}, \tag{4.6d}$$

$$r_3 = \left(2\sqrt{(\alpha^2+\omega^2)\left(\omega^2+\alpha^2\epsilon^2\right)} + 2\alpha^2\epsilon - 2\omega^2\right)^{\frac{1}{2}} c_{\tau} C_p \epsilon^{\delta_p}, \tag{4.6e}$$

$$r_4 = \sqrt{(\alpha^2+\omega^2)\left(\omega^2+\alpha^2\epsilon^2\right)}. \tag{4.6f}$$

Lemma 4.2. *Under the asymptotic assumptions mentioned above, the asymptotic* *expressions of* $R(\omega,0,p_0^*,q_0^*)$ *for* $\omega=0$ *and* $\omega\to\infty$ *are given by*

$$R(0,0,p_0^*,q_0^*) = 1-\frac{4\alpha}{C_p c_T}\epsilon^{\frac{1}{2}-\delta_p}+\mathcal{O}\left(\epsilon^{1-2\delta_p}\right), \tag{4.7}$$

$$R(\infty,0,p_0^*,q_0^*) = \lim_{\omega\to\infty} R(\omega,0,p_0^*,q_0^*) = 1-\frac{4}{C_q c_T}\epsilon^{\delta_q}+\mathcal{O}\left(\epsilon^{2\delta_q}\right). \tag{4.8}$$

Proof. Substituting $\omega=0$ into equation (4.6a) leads to

$$R(0,0,p_0^*,q_0^*) = \frac{C_p^2c_T^2\epsilon^{2\delta_p}-2C_pc_T\alpha\epsilon^{\frac{1}{2}+\delta_p}+\epsilon\alpha^2}{C_p^2c_T^2\epsilon^{2\delta_p}+2C_pc_T\alpha\epsilon^{\frac{1}{2}+\delta_p}+\epsilon\alpha^2} = 1-\frac{4\alpha}{C_pc_T}\epsilon^{\frac{1}{2}-\delta_p}+\mathcal{O}\left(\epsilon^{1-2\delta_p}\right).$$

Similarly, for the limit of $R(\omega,0,p_0^*,q_0^*)$ as $\omega\to\infty$, we factor out the highest power of ω in its expression to arrive at

$$R(\infty,0,p_0^*,q_0^*) = \lim_{\omega\to\infty} R(\omega,0,p_0^*,q_0^*) = \frac{C_q^2c_T^2\epsilon^{-2\delta_q}-2C_qc_T\epsilon^{-\delta_q}+1}{C_q^2c_T^2\epsilon^{-2\delta_q}+2C_qc_T\epsilon^{-\delta_q}+1} = 1-\frac{4}{C_qc_T}\epsilon^{\delta_q}+\mathcal{O}\left(\epsilon^{2\delta_q}\right)$$

completing the proof of this lemma. ∎

LEMMA 4.3. *The exponents* δ_p *and* δ_q*, and coefficients* C_p *and* C_q*, of* p_0^* *and* q_0^* *are related via the equations* $\delta_p+\delta_q=\frac{1}{2}$ *and* $C_p=C_q\alpha$.

Proof. The solution of the min-max problem (4.2) is given by solving the equioscillation equations (4.3a). Comparing the exponents and coefficients of $R(0,0,p_0^*,q_0^*) = |\rho_{\text{opt}}(0,0,p_0^*,q_0^*)|$ and $R(\infty,0,p_0^*,q_0^*) = \lim_{\omega\to\infty}|\rho_{\text{opt}}(\infty,0,p_0^*,q_0^*)|$ gives the result. ∎

LEMMA 4.4. *The constants in the expressions of* $\overline{\omega}=C_\omega\epsilon^{\delta_\omega}$ *are given by* $C_\omega=\alpha$ *and* $\delta_\omega=\frac{1}{2}$*. Moreover, we have either*

$$R(\overline{\omega},0,p_0^*,q_0^*) = 1-4\sqrt{2}C_qc_T\epsilon^{\frac{1}{4}-\delta_q}+\mathcal{O}(\epsilon^{\frac{1}{2}}),\quad or \tag{4.9}$$

$$R(\overline{\omega},0,p_0^*,q_0^*) = 1-\frac{2\sqrt{2}}{C_qc_T}\epsilon^{\delta_q-\frac{1}{4}}+\mathcal{O}(\epsilon^{2\delta_q-\frac{1}{2}}). \tag{4.10}$$

Proof. Recall the expression for $R(\omega,0,p_0^*,q_0^*)$ given in (4.6a). We first reduce the expression for r_2, r_3 and r_4 in (4.6d)-(4.6f). We use these expressions to find the constants C_ω and δ_ω where $\overline{\omega}=C_\omega\epsilon^{\delta_\omega}$, with $0<\delta_\omega<1$. By direct computation, we obtain $r_4=\omega\alpha+\mathcal{O}\left(\omega^3\right)$, $r_2=\sqrt{2}\sqrt{\alpha}C_qc_T\omega^{\frac{3}{2}}\epsilon^{-\delta_q}+\mathcal{O}(\omega^{\frac{5}{2}})$ and $r_3=\sqrt{2}\sqrt{\alpha}C_pc_T\omega^{\frac{1}{2}}\epsilon^{\delta_p}+\mathcal{O}(\omega^{\frac{3}{2}})$, which leads to

$$R(\omega,0,p_0^*,q_0^*) = \frac{r_0+r_1-r_2-r_3+r_4}{r_0+r_1+r_2+r_3+r_4} =: \frac{A(\omega)}{B(\omega)},\ \text{with} \tag{4.11a}$$

$$A(\omega) = \frac{C_q^2c_T^2\omega^2}{\epsilon^{2\delta_q}}+C_p^2c_T^2\epsilon^{2\delta_p}+\alpha\omega-\frac{\sqrt{2}\sqrt{\alpha}C_qc_T\omega^{\frac{3}{2}}}{\epsilon^{\delta_q}}-\sqrt{2}\sqrt{\alpha}C_pc_T\omega^{\frac{1}{2}}\epsilon^{\delta_p}+\mathcal{O}(\omega^{\frac{5}{2}}), \tag{4.11b}$$

$$B(\omega) = \frac{C_q^2c_T^2\omega^2}{\epsilon^{2\delta_q}}+C_p^2c_T^2\epsilon^{2\delta_p}+\alpha\omega+\frac{\sqrt{2}\sqrt{\alpha}C_qc_T\omega^{\frac{3}{2}}}{\epsilon^{\delta_q}}+\sqrt{2}\sqrt{\alpha}C_pc_T\omega^{\frac{1}{2}}\epsilon^{\delta_p}+\mathcal{O}(\omega^{\frac{5}{2}}). \tag{4.11c}$$

We now need to consider different cases depending on which of the positive terms in the numerator $A(\omega)$ are dominant. Let us first consider that the first positive term in the numerator $\frac{C_q^2c_T^2\omega^2}{\epsilon^{2\delta_q}}$ is dominant. This reduces $A(\omega)$ and $B(\omega)$ to

$$A(\omega) = \frac{C_q^2c_T^2\omega^2}{\epsilon^{2\delta_q}}-\frac{\sqrt{2}\sqrt{\alpha}C_qc_T\omega^{\frac{3}{2}}}{\epsilon^{\delta_q}}-\sqrt{2}\sqrt{\alpha}C_pc_T\omega^{\frac{1}{2}}\epsilon^{\delta_p}+\mathcal{O}(\omega^{\frac{5}{2}}),$$

$$B(\omega) = \frac{C_q^2c_T^2\omega^2}{\epsilon^{2\delta_q}}+\frac{\sqrt{2}\sqrt{\alpha}C_qc_T\omega^{\frac{3}{2}}}{\epsilon^{\delta_q}}+\sqrt{2}\sqrt{\alpha}C_pc_T\omega^{\frac{1}{2}}\epsilon^{\delta_p}+\mathcal{O}(\omega^{\frac{5}{2}}).$$

The expression for $\overline{\omega}$ is obtained by solving the equation $\frac{\partial}{\partial\omega}R(\omega,0,p_0^*,q_0^*) = 0$, i.e $\frac{\partial B}{\partial\omega}A - \frac{\partial A}{\partial\omega}B = 0$, and we find by differentiating

$$\frac{\partial B}{\partial\omega}A - \frac{\partial A}{\partial\omega}B = \frac{\sqrt{2}\sqrt{\alpha}C_q^3c_{\scriptscriptstyle T}^3\omega^{\frac{5}{2}}}{\epsilon^{3\delta_q}} + \frac{3\sqrt{2}\sqrt{\alpha}C_pC_q^2c_{\scriptscriptstyle T}^3\omega^{\frac{3}{2}}\epsilon^{\delta_p}}{\epsilon^{2\delta_q}},$$

which cannot be 0 since $\omega > 0$. This is a contraction to our assumption that the first term is dominant. A similar contradiction is obtained if we consider that the second term $C_p^2c_{\mathrm{T}}^2\epsilon^{2\delta_p}$ to be dominant. Now assume that the third term $\alpha\omega$ is dominant. This reduces $A(\omega)$ and $B(\omega)$ to

$$A(\omega) = \alpha\omega - \frac{\sqrt{2}\sqrt{\alpha}C_qc_{\scriptscriptstyle T}\omega^{\frac{3}{2}}}{\epsilon^{\delta_q}} - \sqrt{2}\sqrt{\alpha}C_pc_{\scriptscriptstyle T}\omega^{\frac{1}{2}}\epsilon^{\delta_p} + \mathcal{O}(\omega^{\frac{5}{2}}),$$

$$B(\omega) = \alpha\omega + \frac{\sqrt{2}\sqrt{\alpha}C_qc_{\scriptscriptstyle T}\omega^{\frac{3}{2}}}{\epsilon^{\delta_q}} + \sqrt{2}\sqrt{\alpha}C_pc_{\scriptscriptstyle T}\omega^{\frac{1}{2}}\epsilon^{\delta_p} + \mathcal{O}(\omega^{\frac{5}{2}}).$$

Differentiating these expressions with respect to ω yields

$$\frac{\partial B}{\partial\omega}A - \frac{\partial A}{\partial\omega}B = \frac{-\sqrt{2}c_{\scriptscriptstyle T}C_q\alpha^{\frac{3}{2}}\omega^{\frac{3}{2}}}{\epsilon^{\delta_q}} + \alpha^{\frac{3}{2}}\sqrt{2}c_{\scriptscriptstyle T}C_p\omega^{\frac{1}{2}}\epsilon^{\delta_p} = 0,$$

and thus $\overline{\omega} = \frac{C_p}{C_q}\epsilon^{\delta_q+\delta_p}$. Using the relations in Lemma 4.3, leads to $\overline{\omega} = \alpha\epsilon^{\frac{1}{2}}$. Next, we derive an asymptotic expression for $R(\overline{\omega},0,p_0^*,q_0^*)$. Since $\delta_p + \delta_q = \frac{1}{2}$, we have $\delta_p - \frac{1}{4} = \frac{1}{4} - \delta_q$. Therefore, after a short computation, we get

$$R(\overline{\omega},0,p_0^*,q_0^*) = 1 - 4\sqrt{2}C_qc_{\scriptscriptstyle T}\epsilon^{\frac{1}{4}-\delta_q} + \mathcal{O}(\epsilon^{\frac{1}{2}}).$$

Note however that we have not yet covered all cases. Consider the fourth case where we assume that the sum of first two positive terms in $A(\omega)$, that is, $\frac{C_q^2c_{\mathrm{T}}^2\omega^2}{\epsilon^{2\delta_q}} + C_p^2c_{\mathrm{T}}^2\epsilon^{2\delta_p}$ is dominant. Proceeding as above, we obtain $\overline{\omega} = \alpha\epsilon^{\frac{1}{2}}$, and hence using the relations $\delta_p + \delta_q = \frac{1}{4}$ and $C_p = \alpha C_q$, we get in this case

$$R(\overline{\omega},0,p_0^*,q_0^*) = 1 - \frac{2\sqrt{2}}{C_qc_{\scriptscriptstyle T}}\epsilon^{\delta_q-\frac{1}{4}} + \mathcal{O}(\epsilon^{2\delta_q-\frac{1}{2}}).$$

Now consider the fifth case where the sum $\frac{C_q^2c_{\mathrm{T}}^2\omega^2}{\epsilon^{2\delta_q}} + \alpha\omega$ is larger. This is possible only when $2\delta_\omega - 2\delta_q = \delta_\omega$, that is, $\delta_\omega = 2\delta_q$. Further calculating $\frac{\partial B}{\partial\omega}A - \frac{\partial A}{\partial\omega}B = 0$ again yields $\delta_\omega = \delta_p + \delta_q = \frac{1}{2}$. We thus have $\delta_p = \delta_q = \frac{1}{4}$. Under these conditions all terms in the expression of $A(\omega)$ are $\mathcal{O}(\epsilon^{\frac{1}{2}})$. This is a contradiction. We arrive at the same contradiction when we consider the remaining cases, namely when the terms $C_p^2c_{\mathrm{T}}^2\epsilon^{2\delta_p} + \alpha\omega$ or $\frac{C_q^2c_{\mathrm{T}}^2\omega^2}{\epsilon^{2\delta_q}} + C_p^2c_{\mathrm{T}}^2\epsilon^{2\delta_p} + \alpha\omega$ are dominant. This completes the proof.□

Now we have the required relations to give an asymptotic expression for the optimized parameters p_0^* and q_0^*.

THEOREM 4.5. *The asymptotic solution of the min-max problem* (4.2) *for* $l = 0$ *and small* $\epsilon = \frac{\beta}{\alpha}$ *is given by*

$$p_0^* = \left(\frac{\alpha}{2^{\frac{1}{4}}c_{\scriptscriptstyle T}}\right)\epsilon^{\frac{3}{8}}, \quad \textit{and} \quad q_0^* = \left(\frac{1}{2^{\frac{1}{4}}c_{\scriptscriptstyle T}}\right)\epsilon^{-\frac{1}{8}}. \tag{4.12}$$

Proof. We first compare the exponents of the dominant terms in $R(\infty, 0, p_0^*, q_0^*)$ and $R(\varpi, 0, p_0^*, q_0^*)$, and since there are two expressions for $R(\varpi, 0, p_0^*, q_0^*)$, we need to compare with both: comparing with (4.10), we obtain $\delta_q = \delta_q - \frac{1}{4}$, which is a contradiction; comparing with (4.9) results in $\frac{1}{4} - \delta_q = \delta_q$, i.e. $\delta_q = \frac{1}{8}$. Similarly, comparing their coefficients leads to $C_q = \frac{2^{-\frac{1}{4}}}{c_T}$. Finally, the constants C_p and δ_p are obtained using the relations $C_p = C_q\alpha$ and $\delta_p + \delta_q = \frac{1}{2}$ derived in Lemma 4.3. ∎

4.2. The case with overlap. It is well known that overlap leads to increased convergence rates for both SWR and OSWR. In this section, we derive expressions for the optimized p^* and q^* of overlapping OSWR. In the case of overlapping OSWR, we observe numerically that the solution of the min-max problem (4.2) is again given by equioscillation. However, before deriving expressions for the optimized parameters, we analyze the effect of overlap on the convergence factor. Note that the impact of overlap on the convergence of OSWR comes mainly from the term $e^{-2\lambda l}$, with modulus

$$\left|e^{-2\lambda l}\right| = e^{-\frac{l}{c_T}\left(2\sqrt{(\alpha^2+\omega^2)(\alpha^2\epsilon^2+\omega^2)}+2\epsilon\alpha^2-2\omega^2\right)^{\frac{1}{2}}}.$$

LEMMA 4.6. *For small and large ω, we have the expansions*

$$\left|e^{-2\lambda l}\right| = 1 - \frac{l\sqrt{2}\sqrt{\alpha}}{c_T}\omega^{\frac{1}{2}} + \mathcal{O}(\omega), \quad \left|e^{-2\lambda l}\right| = e^{-\frac{\alpha(1+\epsilon)\,l}{c_T}} + \mathcal{O}\left(\frac{1}{\omega^2}\right). \tag{4.13}$$

Proof. For small ω, using the expansion for r_4 in Subsection 4.1, we get

$$\lim_{\omega\to 0}\left|e^{-2\lambda l}\right| = e^{-\frac{l}{c_T}\left(2r_4+2\epsilon\alpha^2-2\omega^2\right)^{\frac{1}{2}}} = 1 - \frac{l\sqrt{2}\sqrt{\alpha}}{c_T}\omega^{\frac{1}{2}} + \mathcal{O}\left(\omega\right),$$

For large ω, a direct expansion about $\omega = \infty$ yields the second result. ∎

From Lemma 4.6, we see that for small ω, the effect of overlap is negligible since $\lim_{\omega\to 0}\left|e^{-2\lambda l}\right| \to 1$. However, the situation changes for large ω. On the one hand, for small overlap, i.e. for l such that $\frac{\alpha(1+\epsilon)l}{c_T} < 1$ to be precise, a Taylor expansion around $l = 0$ leads to

$$\lim_{l\to 0}\left(\lim_{\omega\to\infty}\left|e^{-2\lambda l}\right|\right) = 1 - \frac{\alpha l}{c_T} + \mathcal{O}\left(l^2\right) + \mathcal{O}\left(\frac{1}{\omega^2}\right), \tag{4.14}$$

which shows that small overlap hardly affects the convergence factor even for higher frequencies. On the other hand large overlap drastically reduces the convergence factor because $e^{-\frac{\alpha(1+\epsilon)\,l}{c_T}} \to 0$ for large l.

Thus in the case of overlapping OSWR, we observe two different types of equioscillation. For small overlap, the equioscillation occurs between $\omega = 0$, $\omega = \widetilde{\omega}_1$, and $\omega = \omega_{\max}$ with $0 < \widetilde{\omega}_1 < \omega_{\max}$ and large $\omega_{\max} \to \infty$. While for large overlap, equioscillation is observed between $\omega = 0$, $\omega = \widetilde{\omega}_1$, and $\omega = \widetilde{\omega}_2$, where $0 < \widetilde{\omega}_1 < \widetilde{\omega}_2 < \omega_{\max} < \infty$. We further observe that the optimized parameters p^* and q^* are positive with $p^*, \widetilde{\omega}_1, \widetilde{\omega}_2 \to 0$, while $q^* \to \infty$ as $\epsilon \to 0$. We thus assume $p^* = \widetilde{C}_p\epsilon^{\widetilde{\delta}_p}$, $\widetilde{\omega}_1 = \widetilde{C}_\omega\epsilon^{\widetilde{\delta}_\omega}$, $\widetilde{\omega}_2 = \widetilde{C}_m\epsilon^{\widetilde{\delta}_m}$ and $q^* = \widetilde{C}_q\epsilon^{-\widetilde{\delta}_q}$, where all constants are greater than 0. Let us again denote by $R(\omega, l, p, q)$ the modulus of convergence factor, i.e. $R(\omega, l, p, q) := |\rho_{\text{opt}}(\omega, l, p, q)|$.

LEMMA 4.7. *For OSWR with overlap, $l \geq 0$, the asymptotic expansion of the convergence factor modulus $R(\omega, l, p^*, q^*)$ for small ω is given by*

$$R(0, l, p^*, q^*) = 1 - \frac{4\alpha}{\widetilde{C}_p c_{\scriptscriptstyle T}} \epsilon^{\frac{1}{2} - \widetilde{\delta}_p} + \mathcal{O}\left(\epsilon^{1-2\widetilde{\delta}_p}\right). \tag{4.15}$$

For large ω, the corresponding expansion is

$$R(\omega, l, p^*, q^*) = \left(1 - \frac{4}{\widetilde{C}_q c_{\scriptscriptstyle T}} \epsilon^{\widetilde{\delta}_q} + \mathcal{O}(\epsilon^{2\widetilde{\delta}_q})\right) \left(e^{-\frac{\alpha(1+\epsilon)\, l}{c_T}} + \mathcal{O}\left(\frac{1}{\omega^2}\right)\right). \tag{4.16}$$

Proof. To obtain (4.15), it suffices to use (4.7) and (4.13) for ω small. Similarly, (4.16) is obtained by multiplying the expansions in (4.13) for large ω and (4.8). ∎

Now we derive asymptotic expressions for $\widetilde{\omega}_1$ and $\widetilde{\omega}_2$, where $0 < \widetilde{\omega}_1 < \widetilde{\omega}_2 < \omega_{\max} < \infty$. Since $\widetilde{\omega}_1, \widetilde{\omega}_2 \to 0$, the effect of overlap is given by the asymptotic expansion (4.13) for ω small.

LEMMA 4.8. *For $l > 0$, $\widetilde{\omega}_1$ and $\widetilde{\omega}_2$ are given by $\widetilde{\omega}_1 = \frac{\widetilde{C}_p}{\widetilde{C}_q} \epsilon^{\widetilde{\delta}_q + \widetilde{\delta}_p}$ and $\widetilde{\omega}_2 = \frac{2}{l\widetilde{C}_q} \epsilon^{\widetilde{\delta}_q}$, and the convergence factor at $\widetilde{\omega}_1$ and $\widetilde{\omega}_2$ satisfies*

$$R(\widetilde{\omega}_1, l, p^*, q^*) = 1 - \frac{4\sqrt{2} c_{\scriptscriptstyle T} \sqrt{\widetilde{C}_q \widetilde{C}_p}}{\sqrt{\alpha}} \epsilon^{\frac{\widetilde{\delta}_p}{2} - \frac{\widetilde{\delta}_q}{2}} + \mathcal{O}(\epsilon^{\widetilde{\delta}_p - \widetilde{\delta}_q}), \tag{4.17}$$

$$R(\widetilde{\omega}_2, l, p^*, q^*) = 1 - \frac{4\sqrt{\alpha}\sqrt{l}}{c_{\scriptscriptstyle T} \sqrt{\widetilde{C}_q}} \epsilon^{\frac{\widetilde{\delta}_q}{2}} + \mathcal{O}(\epsilon^{\widetilde{\delta}_q}). \tag{4.18}$$

Proof. Recall from (4.11) and (4.13) that for small ω,

$$\begin{aligned}
R(\omega, l, p^*, q^*) &= R(\omega, 0, p^*, q^*)\, |e^{-2\lambda l}| \\
&= \left(\frac{\frac{\widetilde{C}_q^2 c_{\mathrm{T}}^2 \omega^2}{\epsilon^{2\widetilde{\delta}_q}} + \widetilde{C}_p^2 c_{\mathrm{T}}^2 \epsilon^{2\widetilde{\delta}_p} + \alpha\omega - \frac{\sqrt{2}\sqrt{\alpha}\widetilde{C}_q c_T \omega^{\frac{3}{2}}}{\epsilon^{\widetilde{\delta}_q}} - \sqrt{2}\sqrt{\alpha}\widetilde{C}_p c_T \omega^{\frac{1}{2}} \epsilon^{\widetilde{\delta}_p} + \mathcal{O}(\omega^{\frac{5}{2}})}{\frac{\widetilde{C}_q^2 c_{\mathrm{T}}^2 \omega^2}{\epsilon^{2\widetilde{\delta}_q}} + \widetilde{C}_p^2 c_{\mathrm{T}}^2 \epsilon^{2\widetilde{\delta}_p} + \alpha\omega + \frac{\sqrt{2}\sqrt{\alpha}\widetilde{C}_q c_T \omega^{\frac{3}{2}}}{\epsilon^{\widetilde{\delta}_q}} + \sqrt{2}\sqrt{\alpha}\widetilde{C}_p c_T \omega^{\frac{1}{2}} \epsilon^{\widetilde{\delta}_p} + \mathcal{O}(\omega^{\frac{5}{2}})} \right) \\
&\quad \times \left(1 - \frac{l\sqrt{2}\sqrt{\alpha}}{c_T} \omega^{\frac{1}{2}} + \mathcal{O}(\omega)\right).
\end{aligned}$$

Similar to proof of Lemma 4.4, we consider different cases depending on which of the positive terms in the numerator of $R(\omega, l, p^*, q^*)$ are dominant. Let us first consider the case when the term $\alpha\omega$ is dominant. Then $R(\omega, l, p^*, q^*)$ reduces to

$$\begin{aligned}
R(\omega, l, p^*, q^*) &= \left(\frac{\alpha\omega - \frac{\sqrt{2}\sqrt{\alpha}\widetilde{C}_q c_T \omega^{\frac{3}{2}}}{\epsilon^{\widetilde{\delta}_q}} - \sqrt{2}\sqrt{\alpha}\widetilde{C}_p c_T \omega^{\frac{1}{2}} \epsilon^{\widetilde{\delta}_p} + \mathcal{O}(\omega^{\frac{5}{2}})}{\alpha\omega + \frac{\sqrt{2}\sqrt{\alpha}\widetilde{C}_q c_T \omega^{\frac{3}{2}}}{\epsilon^{\widetilde{\delta}_q}} + \sqrt{2}\sqrt{\alpha}\widetilde{C}_p c_T \omega^{\frac{1}{2}} \epsilon^{\widetilde{\delta}_p} + \mathcal{O}(\omega^{\frac{5}{2}})} \right) \left(1 - \frac{l\sqrt{2}\sqrt{\alpha}}{c_T} \omega^{\frac{1}{2}} + \mathcal{O}(\omega)\right) \\
&= \frac{\alpha\omega - \frac{\sqrt{2}\sqrt{\alpha}\widetilde{C}_q c_T \omega^{\frac{3}{2}}}{\epsilon^{\widetilde{\delta}_q}} - \sqrt{2}\sqrt{\alpha}\widetilde{C}_p c_T \omega^{\frac{1}{2}} \epsilon^{\widetilde{\delta}_p} - \frac{\sqrt{2}\, l\, \alpha^{\frac{3}{2}} \omega^{\frac{3}{2}}}{c_T} + \mathcal{O}(\omega^2)}{\alpha\omega + \frac{\sqrt{2}\sqrt{\alpha}\widetilde{C}_q c_T \omega^{\frac{3}{2}}}{\epsilon^{\widetilde{\delta}_q}} + \sqrt{2}\sqrt{\alpha}\widetilde{C}_p c_T \omega^{\frac{1}{2}} \epsilon^{\widetilde{\delta}_p} + \mathcal{O}(\omega^{\frac{5}{2}})}.
\end{aligned}$$

Differentiating as before $R(\omega, l, p^*, q^*)$ with respect to ω and equating dominant terms with zero gives

$$\sqrt{2}\alpha^{\frac{3}{2}} \widetilde{C}_p c_{\scriptscriptstyle T} \epsilon^{\widetilde{\delta}_p} \sqrt{\omega} - \frac{\sqrt{2}\alpha^{\frac{3}{2}} c_{\scriptscriptstyle T} \widetilde{C}_q \omega^{\frac{3}{2}}}{\epsilon^{\widetilde{\delta}_q}} = 0 \quad \Longrightarrow \widetilde{\omega}_1 = \frac{\widetilde{C}_p}{\widetilde{C}_q} \epsilon^{\widetilde{\delta}_p + \widetilde{\delta}_q}.$$

Substituting $\widetilde{\omega}_1$ into the above expression of $R(\omega, l, p^*, q^*)$ leads then to (4.17). Next, we consider the case in which the term $\frac{\widetilde{C}_q^2 c_{\mathrm{T}}^2 \omega^2}{\epsilon^{2\widetilde{\delta}_q}}$ is dominant. This is possible only when $\widetilde{\delta}_\omega < \widetilde{\delta}_p + \widetilde{\delta}_q$ and hence $R(\omega, l, p^*, q^*)$ becomes

$$R(\omega, l, p^*, q^*) = \left(\frac{\frac{\widetilde{C}_q^2 c_{\mathrm{T}}^2 \omega^2}{\epsilon^{2\widetilde{\delta}_q}} - \frac{\sqrt{2}\sqrt{\alpha}\widetilde{C}_q c_T \omega^{\frac{3}{2}}}{\epsilon^{\widetilde{\delta}_q}} + \mathcal{O}(\omega^{\frac{5}{2}})}{\frac{\widetilde{C}_q^2 c_{\mathrm{T}}^2 \omega^2}{\epsilon^{2\widetilde{\delta}_q}} + \frac{\sqrt{2}\sqrt{\alpha}\widetilde{C}_q c_T \omega^{\frac{3}{2}}}{\epsilon^{\widetilde{\delta}_q}} + \mathcal{O}(\omega^{\frac{5}{2}})} \right) \left(1 - \frac{l\sqrt{2}\sqrt{\alpha}}{c_T}\omega^{\frac{1}{2}} + \mathcal{O}(\omega)\right). \tag{4.19}$$

Differentiating $R(\omega, l, p^*, q^*)$ with respect to ω and equating dominant terms to zero leads to

$$\frac{\widetilde{C}_q^3 c_T^3 \sqrt{2\alpha}\omega^{\frac{5}{2}}}{\epsilon^{3\widetilde{\delta}_q}} - \frac{\widetilde{C}_q^4 c_T^3 \sqrt{2\alpha} l \omega^{\frac{7}{2}}}{2\epsilon^{4\widetilde{\delta}_q}} = 0 \quad \Longrightarrow \widetilde{\omega}_2 = \frac{2}{l\,\widetilde{C}_q}\epsilon^{\widetilde{\delta}_q}.$$

Substituting $\omega = \widetilde{\omega}_2$ into (4.19) yields after a short calculation (4.18). For the remaining cases, we arrive at a contradiction which similarly to the ones in the proof of Lemma 4.4. ∎

REMARK. *It is easy to see that $\widetilde{\omega}_2 \to \infty$ as the overlap $l \to 0$. Let us denote by l^* the overlap when the two types of equioscillations for the overlapping OSWR match, and distinguish the optimized parameters p^*, q^* for two different cases of equioscillation. Let p_s^* and q_s^* denote optimized parameters for small overlap and p_L^*, q_L^* the ones for large overlap. An explicit relation for l^* can be found by equating $R(\widetilde{\omega}_2, l^*, p_L^*, q_L^*) = \lim_{\omega\to\infty} R(\omega, l^*, p_s^*, q_s^*)$.*

THEOREM 4.9. *For small overlap $l \le \min\left\{\frac{c_T}{\alpha+\beta}, l^*\right\}$, and small $\epsilon = \frac{\beta}{\alpha}$, the optimized parameters p_s^* and q_s^* are uniquely given by*

$$p_s^* = \left(\frac{\alpha}{2^{\frac{1}{4}} c_T}\right)\epsilon^{\frac{3}{8}}, \quad \textit{and} \quad q_s^* = \left(\frac{1}{2^{\frac{1}{4}} c_T}\right)\epsilon^{-\frac{1}{8}}. \tag{4.20}$$

Proof. Substituting the Taylor expansion of $\lim_{\omega\to\infty}|e^{-2\lambda l}|$ for small overlap (4.14) into (4.16) gives

$$\begin{aligned} R(\omega, l, p_s^*, q_s^*) &= \left(1 - \tfrac{4}{\widetilde{C}_q c_T}\epsilon^{\widetilde{\delta}_q} + \mathcal{O}(\epsilon^{2\widetilde{\delta}_q})\right)\left(1 - \tfrac{\alpha l}{c_T} + \mathcal{O}\left(l^2\right) + \mathcal{O}\left(\tfrac{1}{\omega^2}\right)\right) \\ &= \left(1 - \tfrac{4}{\widetilde{C}_q c_T}\epsilon^{\widetilde{\delta}_q} + \mathcal{O}(\epsilon^{2\widetilde{\delta}_q})\right). \end{aligned}$$

Comparing exponents of dominant terms of $\lim_{\omega\to\infty} R(\omega, l, p_s^*, q_s^*)$, $R(0, l, p_s^*, q_s^*)$ and $R(\widetilde{\omega}_1, l, p_s^*, q_s^*)$ then yields $\frac{1}{2} - \widetilde{\delta}_p = \widetilde{\delta}_q = \frac{\widetilde{\delta}_p}{2} - \frac{\widetilde{\delta}_q}{2}$, that is, $\widetilde{\delta}_p = \frac{3}{8}$ and $\widetilde{\delta}_q = \frac{1}{8}$. Similarly, comparing coefficients of these dominant terms, we obtain $\frac{4}{\widetilde{C}_q c_T} = \frac{4\alpha}{\widetilde{C}_p c_T} = \frac{4\sqrt{2}\sqrt{\widetilde{C}_q \widetilde{C}_p} c_T}{\sqrt{\alpha}}$, which on solving leads to (4.20). ∎

Note that for small overlap $l < \frac{c_T}{\alpha+\beta}$, the optimizing parameters p_s^* and q_s^* coincide with the optimizing parameters p_0^* and q_0^* of the nonoverlapping case.

We now study the final case, that is, when the overlap is large.

THEOREM 4.10. *For large overlap l and small $\epsilon = \frac{\beta}{\alpha}$, the optimized p_L^* and q_L^* satisfy*

$$p_L^* = \left(\frac{\alpha^4}{2c_T^4\, l}\right)^{\frac{1}{5}}\epsilon^{\frac{2}{5}}, \quad \textit{and} \quad q_L^* = \left(\frac{\alpha^3\, l^3}{4c_T^8}\right)^{\frac{1}{5}}\epsilon^{-\frac{1}{5}}. \tag{4.21}$$

Proof. Comparing the exponents and coefficients of dominant terms in the asymptotic expansions of $R(0,l,p,q)$, $R(\widetilde{\omega}_1,l,p,q)$, and $R(\widetilde{\omega}_2,l,p,q)$, we get two set of equations, $\frac{1}{2}-\widetilde{\delta}_p=\frac{\widetilde{\delta}_q}{2}=\frac{\widetilde{\delta}_p}{2}-\frac{\widetilde{\delta}_q}{2}$ and $\frac{4\alpha}{\widetilde{C}_p c_T}=\frac{4\sqrt{\alpha l}}{c_T\sqrt{\widetilde{C}_q}}=\frac{4\sqrt{2}\sqrt{\widetilde{C}_q\widetilde{C}_p c_T}}{\sqrt{\alpha}}$, which on solving yield (4.21). ∎

5. Time discretization. This section is devoted to the analysis of time discretizations for the telegrapher equation (1.1). To be precise, we construct and analyze the stability and order of fully discrete schemes.

In [1, 14], numerical experiments were performed by solving the system of ODEs (3.1) using Backward Euler. Backward Euler is unconditionally stable, but we have to pay the price of solving large linear systems at each time step. To avoid this, we can apply an explicit time integration scheme, but at the cost of restrictions on the time steps via a CFL condition. It is unclear how the CFL condition would look like for the circuit equations (3.1) and which circuit parameters would affect it. Moreover Backward Euler is only first-order in time, while one can achieve second-order convergence by choosing an appropriate time integration scheme. We try to address these issues by first constructing fully discrete schemes for the telegrapher equation (1.1), and then analyze them. The novelty is that our schemes are based on the circuit equations (3.1).

5.1. Construction of fully discrete schemes. In Section 3, we showed that the circuit equations (3.1) and the telegrapher equation (1.1a) are related via the coupled first-order PDEs (3.2). We now construct different time integration schemes for (1.1a) based on discretizations of (3.2).

Let $\mathrm{V}^n:=\mathrm{V}(x,t_n)$, $\mathrm{I}^n:=\mathrm{I}(x,t_n)$ and $u^n:=u(x,t_n)$ be approximations of the solutions $\mathrm{V}(x,t),\mathrm{I}(x,t)$, and $u(x,t)$ at time $t_n=n\tau$, where τ is the time step. For the fully discrete scheme, we further approximate the space derivative of $u_j^n:=u(x_j,t_n)$ by second-order centered finite differences, $\frac{\partial^2 u_j^n}{\partial x^2}\approx\frac{u_{j+1}^n-2u_j^n+u_{j-1}^n}{h^2}$, where h is the space step.

First, we treat both equations of (3.2) by Backward Euler, $\frac{\mathrm{I}^{n+1}-\mathrm{I}^n}{\tau}=-\frac{1}{\mathrm{L}}\frac{\partial\mathrm{V}^{n+1}}{\partial x}-\alpha\mathrm{I}^{n+1}$ and $\frac{\mathrm{V}^{n+1}-\mathrm{V}^n}{\tau}=-\frac{1}{\mathrm{C}}\frac{\partial\mathrm{I}^{n+1}}{\partial x}-\beta\mathrm{V}^{n+1}$, which can be rearranged to

$$\frac{1}{\mathrm{L}}\frac{\partial\mathrm{V}^{n+1}}{\partial x}=-\frac{\mathrm{I}^{n+1}-\mathrm{I}^n}{\tau}-\alpha\mathrm{I}^{n+1},\quad\text{and}\quad\frac{1}{\mathrm{C}}\frac{\partial\mathrm{I}^{n+1}}{\partial x}=-\frac{\mathrm{V}^{n+1}-\mathrm{V}^n}{\tau}-\beta\mathrm{V}^{n+1}.\tag{5.1}$$

Differentiating the first relation in (5.1) with respect to x and using the second relation in (5.1) leads to

$$\frac{1}{\mathrm{L}}\frac{\partial^2\mathrm{V}^{n+1}}{\partial x^2}=\mathrm{C}\left(\frac{\mathrm{V}^{n+1}-2\mathrm{V}^n+\mathrm{V}^{n-1}}{\tau^2}+(\alpha+\beta)\left(\frac{\mathrm{V}^{n+1}-\mathrm{V}^n}{\tau}\right)+\alpha\beta\mathrm{V}^{n+1}\right).\tag{5.2}$$

We arrive at a similar result for the current I^{n+1} by differentiating the second relation in (5.1) with respect to x and then substituting the first relation in (5.1). Thus, an implicit fully discrete scheme for the telegrapher equation (1.1a) is

$$\frac{u_j^{n+1}-2u_j^n+u_j^{n-1}}{\tau^2}+(\alpha+\beta)\left(\frac{u_j^{n+1}-u_j^n}{\tau}\right)+\alpha\beta u_j^{n+1}=c_{\mathrm{T}}^2\left(\frac{u_{j+1}^{n+1}-2u_j^{n+1}+u_{j-1}^{n+1}}{h^2}\right)+f_j^{n+1},\tag{5.3}$$

where $f_j^n:=f(x_j,t_n)$. Clearly, this scheme is an implicit scheme in time. It is easy to prove using Taylor expansion that this scheme is first order in time and second order in space.

If we apply Backward Euler to the first relation in (5.1) and Forward Euler to the second relation in (5.1), and perform similar steps as above, we arrive at

$$\frac{u_j^{n+1}-2u_j^n+u_j^{n-1}}{\tau^2}+\alpha\left(\frac{u_j^{n+1}-u_j^n}{\tau}\right)+\beta\left(\frac{u_j^{n}-u_j^{n-1}}{\tau}\right)+\alpha\beta u_j^n=c_{\mathrm{T}}^2\left(\frac{u_{j+1}^n-2u_j^n+u_{j-1}^n}{h^2}\right)+f_j^n. \tag{5.4}$$

This scheme is explicit in time but again of first order only, unless $\alpha=\beta=\frac{1}{2}$.

To achieve an explicit scheme of second order in time, we treat the first relation in (5.1) and the second relation in (5.1) differently, namely $\frac{\mathrm{I}^{n+1}-\mathrm{I}^n}{\tau}=-\frac{1}{\mathrm{L}}\frac{\partial \mathrm{V}^n}{\partial x}-\frac{\alpha}{2}(\mathrm{I}^{n+1}+\mathrm{I}^n)$ and $\frac{\mathrm{V}^{n+1}-\mathrm{V}^n}{\tau}=-\frac{1}{\mathrm{C}}\frac{\partial \mathrm{I}^{n+1}}{\partial x}-\frac{\beta}{2}(\mathrm{V}^{n+1}+\mathrm{V}^n)$, which we rearrange into

$$\frac{1}{\mathrm{L}}\frac{\partial \mathrm{V}^n}{\partial x}=-\frac{\mathrm{I}^{n+1}-\mathrm{I}^n}{\tau}-\frac{\alpha}{2}(\mathrm{I}^{n+1}+\mathrm{I}^n),\quad \frac{1}{\mathrm{C}}\frac{\partial \mathrm{I}^{n+1}}{\partial x}=-\frac{\mathrm{V}^{n+1}-\mathrm{V}^n}{\tau}-\frac{\beta}{2}(\mathrm{V}^{n+1}+\mathrm{V}^n). \tag{5.5}$$

Again differentiating the first equation in (5.5) with respect to x and substituting into the second equation in (5.5) yields

$$\frac{1}{\mathrm{L}}\frac{\partial^2 \mathrm{V}^n}{\partial x^2}=\mathrm{C}\left(\frac{\mathrm{V}^{n+1}-2\mathrm{V}^n+\mathrm{V}^{n-1}}{\tau^2}+(\alpha+\beta)\left(\frac{\mathrm{V}^{n+1}-\mathrm{V}^{n-1}}{2\tau}\right)+\frac{\alpha\beta}{4}(\mathrm{V}^{n+1}+2\mathrm{V}^n+\mathrm{V}^{n-1})\right).$$

Thus an explicit scheme for the telegrapher equation (1.1a) which is second order in both time and space is

$$\frac{u_j^{n+1}-2u_j^n+u_j^{n-1}}{\tau^2}+(\alpha+\beta)\Big(\frac{u_j^{n+1}-u_j^{n-1}}{2\tau}\Big)+\alpha\beta\Big(\frac{u_j^{n+1}+2u_j^n+u_j^{n-1}}{4}\Big)=c_{\mathrm{T}}^2\Big(\frac{u_{j+1}^n-2u_j^n+u_{j-1}^n}{h^2}\Big)+f_j^n. \tag{5.6}$$

Proceeding in a similar way, one could construct many further fully discrete schemes, but we focus on two of the above schemes in what follows, (5.3) which is implicit, and (5.6) which is explicit.

5.2. Stability analysis. We use Von Neumann analysis [28] to determine the stability criteria of the fully discrete schemes (5.3) and (5.6), i.e. we study the behavior for a single wave number $k\in\mathbb{R}$. For $i:=\sqrt{-1}$, let the discrete solution be $u_j^n=e^{ikjh}$. Let us denote the amplification factor by $g(k)$. Our aim is to find conditions on τ such that for $u_{j+1}^n=g(k)e^{ikjh}$, $g(k)$ satisfies $|g(k)|\le 1$ for all frequencies $k\in\mathbb{R}$.

To start with, we assume $f\equiv 0$, and then substitute $u_j^n=e^{ikjh}$, $u_j^{n+1}=g(k)e^{ikjh}$, and $u_j^{n-1}=(g(k))^{-1}e^{ikjh}$ into the scheme. The second-order derivative in space term simplifies to

$$\frac{u_{j+1}^n-2u_j^n+u_{j-1}^n}{h^2}=\frac{e^{ikjh}}{h^2}\left(2\cos(kh)-2\right)=:-\tilde{k}_h^2e^{ikjh}, \tag{5.7}$$

where $\tilde{k}_h$ can be considered as the frequency for the semi-discrete system.

THEOREM 5.1. *The fully discrete scheme (5.3) is unconditionally stable for all τ.*

Proof. Substituting (5.7) into scheme (5.3) and factoring out common factors, we get

$$\frac{g(k)-2+(g(k))^{-1}}{\tau^2}+(\alpha+\beta)\left(\frac{g(k)-1}{\tau}\right)+\alpha\beta g(k)=-c_{\mathrm{T}}^2g(k)\tilde{k}_h^2,$$

which can be rewritten as

$$\left(1+(\alpha+\beta)\tau+(\alpha\beta+c_{\mathrm{T}}^2\tilde{k}_h^2)\tau^2\right)g^2(k)-\left(2+(\alpha+\beta)\tau\right)g(k)+1=0.$$

Solving for $g(k)$ yields

$$g_{\pm}(k) = \frac{2+(\alpha+\beta)\tau \pm \sqrt{D}}{2\left(1+(\alpha+\beta)\tau+(\alpha\beta+c_{\text{T}}^2\tilde{k}_h^2)\tau^2\right)}, \quad D := \tau^2\left((\alpha-\beta)^2 - 4c_{\text{T}}^2\tilde{k}_h^2\right).$$

Depending upon the value of $\tilde{k}_h^2$, the discrimant D can be positive or negative. Let the two sets $S_1 \subset \mathbb{R}$ and $S_2 \subset \mathbb{R}$ be such that

$$D = \left\{ \begin{array}{ll} D_+ \geq 0, & \text{for } \tilde{k}_h^2 \in S_1 \\ -D_- < 0, & \text{for } \tilde{k}_h^2 \in S_2 \end{array} \right\}, \tag{5.8}$$

with $D_+ = \tau^2\left((\alpha-\beta)^2 - 4c_{\text{T}}^2\tilde{k}_h^2\right) \geq 0$ and $D_- = -\tau^2\left((\alpha-\beta)^2 - 4c_{\text{T}}^2\tilde{k}_h^2\right) > 0$. We first consider the case when $\tilde{k}_h^2 \in S_1$. Then $|g_+(k)| \leq 1$ if and only if

$$-2\left(1+(\alpha+\beta)\tau+(\alpha\beta+c_{\text{T}}^2\tilde{k}_h^2)\tau^2\right) \leq 2+(\alpha+\beta)\tau+\sqrt{D_+}, \tag{5.9}$$

$$2+(\alpha+\beta)\tau+\sqrt{D_+} \leq 2\left(1+(\alpha+\beta)\tau+(\alpha\beta+c_{\text{T}}^2\tilde{k}_h^2)\tau^2\right). \tag{5.10}$$

The first inequality (5.9) is satisfied trivially. For the second inequality (5.10), we rearrange it and square on both sides to arrive at

$$\begin{aligned} D_+ = \tau^2\left((\alpha-\beta)^2 - 4c_{\text{T}}^2\tilde{k}_h^2\right) &\leq \left((\alpha+\beta)\tau+(\alpha\beta+c_{\text{T}}^2\tilde{k}_h^2)\tau^2\right)^2 \\ \Longleftrightarrow\ 0 \leq \tau^2 &\left(4\alpha\beta+4c_{\text{T}}^2\tilde{k}_h^2+\tau(\alpha+\beta)(\alpha\beta+c_{\text{T}}^2\tilde{k}_h^2)+\tau^2\left(\alpha\beta+c_{\text{T}}^2\tilde{k}_h^2\right)^2\right). \end{aligned}$$

The last inequality is clearly satisfied for all $\tau > 0$. Similarly, $|g_-(k)| \leq 1$ if and only if

$$-2\left(1+(\alpha+\beta)\tau+(\alpha\beta+c_{\text{T}}^2\tilde{k}_h^2)\tau^2\right) \leq 2+(\alpha+\beta)\tau-\sqrt{D_+}, \tag{5.11}$$

$$2+(\alpha+\beta)\tau-\sqrt{D_+} \leq 2\left(1+(\alpha+\beta)\tau+(\alpha\beta+c_{\text{T}}^2\tilde{k}_h^2)\tau^2\right). \tag{5.12}$$

Both inequalities Proof 11 are satisfied for all $\tau > 0$.

We now analyze $|g_{\pm}(k)|$ when $\tilde{k}_h^2 \in S_2$. From (5.8), $\sqrt{D} = i\sqrt{-D_-}$ and hence

$$|g_{\pm}(k)|^2 = \frac{(2+(\alpha+\beta)\tau)^2+D_-}{4\left(1+(\alpha+\beta)\tau+(\alpha\beta+c_{\text{T}}^2\tilde{k}_h^2)\tau^2\right)^2} = \frac{1+(\alpha+\beta)\tau+\left(\alpha\beta+c_{\text{T}}^2\tilde{k}_h^2\right)\tau^2}{\left(1+(\alpha+\beta)\tau+(\alpha\beta+c_{\text{T}}^2\tilde{k}_h^2)\tau^2\right)^2} \leq 1.$$

We therefore have $|g_{\pm}(k)| \leq 1$ for all $\tilde{k}_h \in \mathbb{R}$ and for all $\tau > 0$. ☐

THEOREM 5.2. *The scheme (5.6) is stable under the CFL condition* $\tau \leq \frac{h}{c_T}$.

Proof. Proceeding as in the proof of Theorem 5.1, substituting $u_j^n = e^{ikjh}$, $u_j^{n+1} = g(k)e^{ikjh}$, $u_j^{n-1}(g(k))^{-1}e^{ikjh}$ into the scheme (5.6), and using (5.7) yields

$$(4+2(\alpha+\beta)\tau+\alpha\beta\tau^2)g(k)^2 - 2(4-(\alpha\beta+2c_{\text{T}}^2\tilde{k}_h^2)\tau^2)g(k)+(4-2(\alpha+\beta)\tau+\alpha\beta\tau^2) = 0.$$

Solving this quadratic equation leads to

$$g_{\pm}(k) = \frac{4-(\alpha\beta+2c_{\text{T}}^2\tilde{k}_h^2)\tau^2 \pm \frac{\sqrt{D}}{2}}{4+2(\alpha+\beta)\tau+\alpha\beta\tau^2}, \; D = 16\tau^2((\alpha-\beta)^2 - 4c_{\text{T}}^2\tilde{k}_h^2 + c_{\text{T}}^2\tilde{k}_h^2(\alpha\beta+c_{\text{T}}^2\tilde{k}_h^2)\tau^2). \tag{5.13}$$

Depending on $\tilde{k}_h^2$, D is again either positive or negative, and considering the disjoint sets $S_1, S_2 \subset \mathbb{R}$, such that $D = D_+ \geq 0$ if $\tilde{k}_h^2 \in S_1$ and $D = -D_- < 0$ if $\tilde{k}_h^2 \in S_2$, the expression of $g_\pm(k)$ in (5.13) becomes

$$g_\pm(k) = \begin{cases} \frac{4-\left(\alpha\beta+2c_{\mathrm{T}}^2\tilde{k}_h^2\right)\tau^2 \pm \frac{\sqrt{D_+}}{2}}{4+2(\alpha+\beta)\tau+\alpha\beta\tau^2}, & \text{for } \tilde{k}_h^2 \in S_1, \\ \frac{4-\left(\alpha\beta+2c_{\mathrm{T}}^2\tilde{k}_h^2\right)\tau^2 \pm \frac{\sqrt{D_-}}{2}}{4+2(\alpha+\beta)\tau+\alpha\beta\tau^2}, & \text{for } \tilde{k}_h^2 \in S_2, \end{cases}, \tag{5.14}$$

with

$$D_+ = 16\tau^2\left((\alpha-\beta)^2 - 4c_{\mathrm{T}}^2\tilde{k}_h^2 + c_{\mathrm{T}}^2\tilde{k}_h^2\left(\alpha\beta + c_{\mathrm{T}}^2\tilde{k}_h^2\right)\tau^2\right) \geq 0,$$
$$D_- = -16\tau^2\left((\alpha-\beta)^2 - 4c_{\mathrm{T}}^2\tilde{k}_h^2 + c_{\mathrm{T}}^2\tilde{k}_h^2\left(\alpha\beta + c_{\mathrm{T}}^2\tilde{k}_h^2\right)\tau^2\right) > 0.$$

First, let us assume that $\tilde{k}_h^2 \in S_1$. Then $|g_-(k)| \leq 1$ if and only if

$$-\left(4+2(\alpha+\beta)\tau+\alpha\beta\tau^2\right) \leq 4 - \left(\alpha\beta + 2c_{\mathrm{T}}^2\tilde{k}_h^2\right)\tau^2 - \frac{\sqrt{D_+}}{2}, \tag{5.15}$$

$$4 - \left(\alpha\beta + 2c_{\mathrm{T}}^2\tilde{k}_h^2\right)\tau^2 - \frac{\sqrt{D_+}}{2} \leq 4 + 2(\alpha+\beta)\tau + \alpha\beta\tau^2. \tag{5.16}$$

Equation (5.15) can be rearranged to

$$\frac{\sqrt{D_+}}{2} \leq 8 + 2(\alpha+\beta)\tau - 2c_{\mathrm{T}}^2\tilde{k}_h^2\tau^2. \tag{5.17}$$

Squaring on both sides and simplifying gives

$$\begin{aligned} 0 &\leq \left(8+2(\alpha+\beta)\tau - 2c_{\mathrm{T}}^2\tilde{k}_h^2\tau^2\right)^2 - 4\tau^2\left((\alpha-\beta)^2 - 4c_{\mathrm{T}}^2\tilde{k}_h^2 + c_{\mathrm{T}}^2h^2\left(\alpha\beta + c_{\mathrm{T}}^2\tilde{k}_h^2\right)\right) \\ &= 16 + 8(\alpha+\beta)\tau + 4\left(\alpha\beta - c_{\mathrm{T}}^2\tilde{k}_h^2\right)\tau^2 - 2c_{\mathrm{T}}^2\tilde{k}_h^2(\alpha+\beta)\tau^3 - c_{\mathrm{T}}^2\tilde{k}_h^2\alpha\beta\tau^4 \\ &= (4 - c_{\mathrm{T}}^2\tilde{k}_h^2\tau^2)(2+\beta\tau)(2+\alpha\tau). \end{aligned}$$

The terms $(2+\beta\tau)$ and $(2+\alpha\tau)$ are positive, and hence the CFL stems from the first term, and is given by

$$\tau^2 \leq \frac{4}{c_{\mathrm{T}}^2\tilde{k}_h^2}. \tag{5.18}$$

Condition (5.16) is satisfied for $\tau > 0$, as one can see by rearranging it to $0 \leq 2(\alpha+\beta)\tau + 2(\alpha\beta + c_{\mathrm{T}}^2\tilde{k}_h^2)\tau^2 + \frac{\sqrt{D_+}}{2}$. Next, we find conditions on τ for which $|g_+(k)| \leq 1$ for $\tilde{k}_h^2 \in S_1$. $|g_+(k)| \leq 1$ is satisfied if and only if

$$-\left(4+2(\alpha+\beta)\tau+\alpha\beta\tau^2\right) \leq 4 - \left(\alpha\beta + 2c_{\mathrm{T}}^2\tilde{k}_h^2\right)\tau^2 + \frac{\sqrt{D_+}}{2}, \tag{5.19}$$

$$4 - \left(\alpha\beta + 2c_{\mathrm{T}}^2\tilde{k}_h^2\right)\tau^2 + \frac{\sqrt{D_+}}{2} \leq 4 + 2(\alpha+\beta)\tau + \alpha\beta\tau^2. \tag{5.20}$$

Equation (5.19) can be simplified to $-\left(8+2(\alpha+\beta)\tau - 2c_{\mathrm{T}}^2\tilde{k}_h^2\right) \leq \frac{\sqrt{D_+}}{2}$. From (5.17), we clearly observe that this is true for all $\tau > 0$ and $\tilde{k}_h \in S_1$. Further, simplifying

(5.16) to $\frac{\sqrt{D_+}}{2} \leq 2(\alpha+\beta)\tau + 2\left(\alpha\beta + c_{\mathrm{T}}^2 \tilde{k}_h^2\right)\tau^2$. Squaring on both sides results into

$$\begin{aligned}\left((\alpha-\beta)^2 - 4c_{\mathrm{T}}^2\tilde{k}_h^2 + c_{\mathrm{T}}^2\tilde{k}_h^2\left(\alpha\beta + c_{\mathrm{T}}^2\tilde{k}_h^2\right)\tau^2\right) \\ \leq \left((\alpha+\beta)^2 + 2\tau(\alpha+\beta)\left(\alpha\beta + c_{\mathrm{T}}^2\tilde{k}_h^2\right) + \left(\alpha\beta + c_{\mathrm{T}}^2\tilde{k}_h^2\right)^2\tau^2\right),\end{aligned}$$

which simplifies into

$$0 \leq \left(\alpha\beta + c_{\mathrm{T}}^2\tilde{k}_h^2\right)\left(4 + 2\alpha + \beta\tau + \alpha\beta\tau^2\right).$$

Since all terms are positive, the above inequality is always satisfied.

Next consider the case when $\tilde{k}_h^2 \in S_2$, for which we obtain for all $\tau > 0$

$$\begin{aligned}|g_\pm(k)|^2 &= \left|\frac{4-\left(\alpha\beta+2c_{\mathrm{T}}^2\tilde{k}_h^2\right)\tau^2 + i\frac{\sqrt{D_-}}{2}}{4+2(\alpha+\beta)\tau+\alpha\beta\tau^2}\right|^2 \\ &= \frac{\left(4-\left(\alpha\beta+2c_{\mathrm{T}}^2\tilde{k}_h^2\right)\tau^2\right)^2 - 4\tau^2\left(\alpha-\beta\right)^2 - 4c_{\mathrm{T}}^2\tilde{k}_h^2 + c_{\mathrm{T}}^2\tilde{k}_h^2\left(\alpha\beta+c_{\mathrm{T}}^2\tilde{k}_h^2\right)\tau^2\Big)}{(4+2(\alpha+\beta)\tau+\alpha\beta\tau^2)^2} \\ &= \frac{16-4(\alpha+\beta)^+\alpha^2\beta^2\tau^4}{16+8(\alpha+\beta)\tau+4((\alpha+\beta)^2+2\alpha\beta)\tau^2+4\alpha\beta(\alpha+\beta)\tau^3+\alpha^2\beta^2\tau^4} \leq 1.\end{aligned}$$

The CFL condition for scheme (5.6) is thus given by (5.18). Replacing back the definition of $\tilde{k}_h^2$ from (5.7) into (5.18), we get

$$\tau \leq \frac{2h}{c_{\tau}\sqrt{2(1-\cos(kh))}}.$$

Taking the lowest upper bound and using $0 \leq 2(1-\cos(kh)) \leq 2$ gives the CFL $\tau \leq \frac{h}{c_\tau}$. ∎

6. Numerical Experiments. We show three different numerical experiments to illustrate our theoretical results. We start with validating stability and time convergence of the schemes (5.3), (5.4), and (5.6) for the telegrapher equation (1.1a). Next, we study the performance of SWR and OSWR. Finally, we compare the numerically and asymptotically optimized values of p^* and q^* for both overlapping and nonoverlapping OSWR.

For all our experiments we fix randomly chosen values $\alpha = 1.15$, $\beta = 0.05$, and $c_\tau = 0.7$. The space domain $\Omega = [0,1]$ is split into two overlapping domains $\Omega_1 = [0, 0.5+l]$ and $\Omega_2 = [0.5, 1]$, where l denotes the overlap. The space discretization parameter $h = 0.001$ and the final time $T = 1$ is kept constant. Further, we choose the right hand side $f(x,t)$ such that $u(x,t) = (x-x^2)t^2e^{-t}$ is the exact solution. In the first experiment, we analyze if SWR method influences the stability and order of the fully discrete schemes (5.3), (5.4), and (5.6). For this, we choose the SWR iterations large enough, say 150, so that SWR solution has converged to the discrete solution. Moreover, we also fix the overlap $l = 0.01$. Fig. 6.1 shows the error plots for these schemes. The magenta plot shows that the implicit scheme (5.3) does not need any CFL condition and is stable for all time steps τ, and has order 1 in time. Schemes (5.4) and (5.6) are explicit and are stable when τ satisfies the CFL condition. The vertically dotted line denotes the minimum theoretical τ required for both these schemes to be stable. Clearly, the red and blue plots for schemes (5.4) and (5.6)

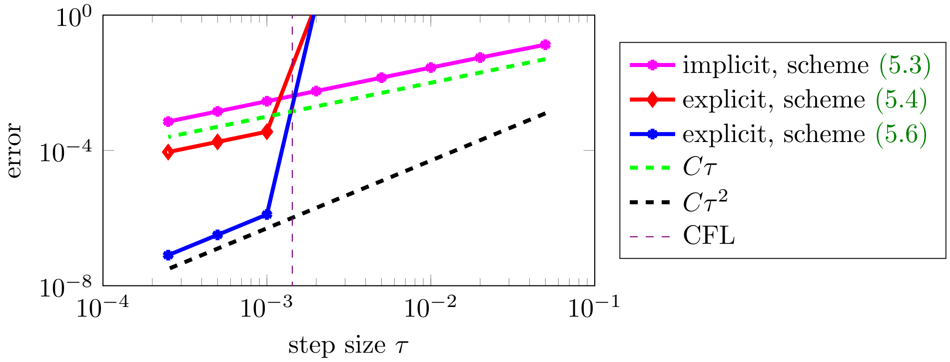

Fig. 6.1: Stability region and time convergence of the fully discrete schemes (5.3), (5.4), and (5.6).

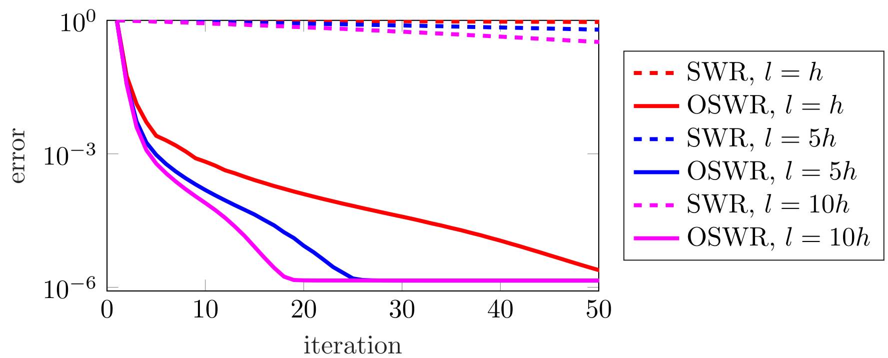

Fig. 6.2: Convergence of SWR and OSWR for different overlaps.

numerically illustrate this. Finally, we observe that (5.4) and (5.6) are of order 1 and 2 in time.

In the second experiment, we fix the time discretization parameter $\tau = 0.001$. We apply SWR and OSWR to the telegrapher equation (1.1a) for different overlaps $l = h, 5h, 10h$. From Fig. 6.2, we see that the convergence of SWR is relatively slow, and while increasing the overlap increases the rate of convergence, as expected, only the use of optimized transmission conditions with asymptotically optimized parameters p^* and q^* makes this into a highly effective solver.

Finally, we illustrate how close the asymptotically optimized p^* and q^* are to the numerically best performing values. For this, we consider the discretization scheme (5.6), and fix overlap to $l = h = 0.001$ and final time $T = 1$. We plot the logarithm (with base 10) of error after 15 iterations of OSWR for different values of p and q in the left plot of Fig. 6.3. The red marker denotes the asymptotically optimized p^*, q^*. We see that the asymptotically optimized p^*, q^* lead to a very small error, close to the best one obtainable by numerical tuning. To illustrate the behavior throughout the iteration, we plot the relative error of OSWR with optimized p^* and q^* in blue and the asymptotically optimized p^*, q^* in red in the right plot of Fig. 6.3. We see that for a small number of iterations, the asymptotically optimized parameters

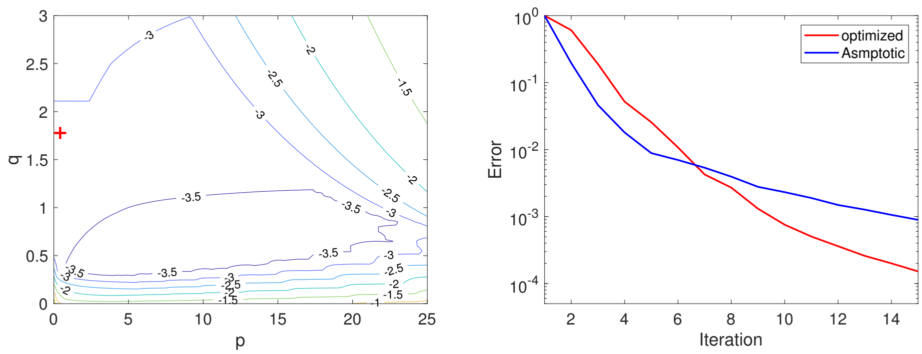

Fig. 6.3: Log10 of the error after 15 iterations (left) with a red marker denoting the asymptotically optimized p^* and q^*, and comparison of the convergence of OSWR using the asymptotically and numerically optimized p^* and q^* (right).

even perform better, only for later iterations the numerically optimized ones get to a smaller error. For recent results investigating such differences for a simpler model, namely the heat equation, see [16]. It should be noted that our analysis is based on the Laplace transform over an unbounded domain (i.e., an infinite time interval). However, in Fig. 6.2 and Fig. 6.3, we present convergence rates and errors on a bounded domain with a maximum time T. The observed convergence rates in Fig. 6.2 and in the right plot of Fig. 6.3 demonstrate and validate our proved results and findings; nevertheless, the convergence behavior is more complex than it appears and deserves further investigations; we refer to [16], where various convergence regimes have been discovered and analyzed for a simpler model to better understand the differences in the convergence behaviors we also observe in Fig. 6.2 and in the right plot of Fig. 6.3.

7. Conclusion.

We proposed and analyzed both overlapping and nonoverlapping SWR and OSWR methods for the telegrapher equation. For OSWR, we used first-order transmission conditions and derived explicit asymptotic expressions for optimized parameters depending on the overlap and the problem parameters. We proved that adding overlap increases the convergence rate of these methods, but the impact of using optimized transmission conditions is far more important than that of the overlap. A further key contribution is the close relation of the telegrapher equation and RLCG transmission lines, leading to an intimate connection between their associated SWR and OSWR convergence factors. This will help circuit designers to easily transfer the analysis and optimized parameters from the telegrapher equation to RLCG circuits, for which general optimized parameters were not known so far. We also constructed fully discrete schemes for the telegrapher equation based on this circuit relation, and analyzed their stability and convergence.

REFERENCES

[1] M. D. Al-Khaleel, M. J. Gander, and A. E. Ruehli, *Optimized waveform relaxation solution of RLCG transmission line type circuits*, in 9th International Conference on Innovations in Information Technology (IIT), IEEE, 2013, pp. 36–140, https://ieeexplore.ieee.org/document/6544407.

[2] M. D. Al-Khaleel, M. J. Gander, and A. E. Ruehli, *Optimization of Transmission Conditions in Waveform Relaxation Techniques for RC Circuits*, SIAM Journal on Numerical Analysis, 52 (2014), pp. 1076–1101, https://doi.org/10.1137/110854187.

[3] D. Bennequin, M. Gander, L. Gouarin, and L. Halpern, *A homographic best approximation problem with application to optimized Schwarz waveform relaxation*, Mathematics of Computation, 265 (2009), pp. 185–223, http://www.jstor.org/stable/40234770.

[4] E. Blayo, L. Halpern, and C. Japhet, *Optimized Schwarz Waveform Relaxation Algorithms with Nonconforming Time Discretization for Coupling Convection-diffusion Problems with Discontinuous Coefficients*, in Domain Decomposition Methods in Science and Engineering XVI, Springer Berlin Heidelberg, 2007, pp. 267–274, https://link.springer.com/chapter/10.1007/978-3-540-34469-8_31.

[5] G. Califano and D. Conte, *Optimal Schwarz waveform relaxation for fractional diffusion-wave equations*, Applied Numerical Mathematics, 127 (2018), pp. 125–141, https://www.sciencedirect.com/science/article/pii/S0168927418300114.

[6] I. C. Cortes Garcia, J. Pade, S. Schöps, C. Strohm, and C. Tischendorf, *Waveform relaxation for field/circuit coupled problems with cutsets of inductances and current sources*, in 2019 International Conference on Electromagnetics in Advanced Applications (ICEAA), IEEE, 2019, pp. 1286–1286, https://ieeexplore.ieee.org/document/8878955.

[7] M. Dehghan and A. Shokri, *A numerical method for solving the hyperbolic telegraph equation*, Numerical Methods for Partial Differential Equations, 24 (2008), pp. 1080–1093, https://onlinelibrary.wiley.com/doi/abs/10.1002/num.20306.

[8] D. J. Evans and H. Bulut, *The numerical solution of the telegraph equation by the alternating group explicit (AGE) method*, International Journal of Computer Mathematics, 80 (2003), pp. 1289–1297, https://doi.org/10.1080/0020716031000112312.

[9] M. J. Gander, *Optimized Schwarz Methods*, SIAM Journal on Numerical Analysis, 44 (2006), pp. 699–731, https://doi.org/10.1137/S0036142903425409.

[10] M. J. Gander, M. Al-Khaleel, and A. E. Ruehli, *Optimized Waveform Relaxation Methods for Longitudinal Partitioning of Transmission Lines*, IEEE Transactions on Circuits and Systems I: Regular Papers, 56 (2009), pp. 1732–1743, https://ieeexplore.ieee.org/document/4663663.

[11] M. J. Gander and L. Halpern, *Optimized Schwarz Waveform Relaxation Methods for Advection Reaction Diffusion Problems*, SIAM Journal on Numerical Analysis, 44 (2007), pp. 666–697, http://www.jstor.org/stable/40232881.

[12] M. J. Gander, L. Halpern, and F. Nataf, *Optimal Schwarz Waveform Relaxation for the One Dimensional Wave Equation*, SIAM Journal on Numerical Analysis, 41 (2003), pp. 1643–1681, https://doi.org/10.1137/S003614290139559X.

[13] M. J. Gander, L. Halpern, and F. Nataf, *Optimal Schwarz Waveform Relaxation for the One Dimensional Wave Equation*, SIAM Journal on Numerical Analysis, 41 (2003), pp. 1643–1681, https://epubs.siam.org/doi/10.1137/S003614290139559X.

[14] M. J. Gander, P. M. Kumbhar, and A. E. Ruehli, *Asymptotic Analysis for Different Partitionings of RLC Transmission Lines*, in Domain Decomposition Methods in Science and Engineering XXV, Springer International Publishing, 2020, pp. 251–259, https://link.springer.com/chapter/10.1007/978-3-030-56750-7_28.

[15] M. J. Gander, P. M. Kumbhar, and A. E. Ruehli, *Asymptotic Analysis for Overlap in Waveform Relaxation Methods for RC Type Circuits*, Journal of Scientific Computing, 84 (2020), https://doi.org/10.1007/s10915-020-01270-5.

[16] M. J. Gander and V. Martin, *Why Fourier mode analysis in time is different when studying Schwarz waveform relaxation*, Journal of Computational Physics, 491 (2023), p. 112316.

[17] F. Gao and C. Chi, *Unconditionally stable difference schemes for a one-space-dimensional linear hyperbolic equation*, Applied Mathematics and Computation, 187 (2007), pp. 1272–1276, https://www.sciencedirect.com/science/article/pii/S0096300306012653.

[18] C.-W. Ho, A. Ruehli, and P. Brennan, *The modified nodal approach to network analysis*, IEEE Transactions on Circuits and Systems, 22 (1975), pp. 504–509, https://ieeexplore.ieee.org/document/1084079.

[19] P. M. Kumbhar, *Asymptotic analysis of optimized waveform relaxation methods for RC circuits and RLCG transmission lines*, PhD thesis, University of Geneva, 01/28 2020, https://archive-ouverte.unige.ch/unige:136729. ID: unige:136729.

[20] F. Kwok, *Neumann–Neumann Waveform Relaxation for the Time-Dependent Heat Equation*, in Domain Decomposition Methods in Science and Engineering XXI, Springer International Publishing, 2014, pp. 189–198, https://link.springer.com/chapter/10.1007/978-3-319-05789-7_15.

[21] F. Kwok and B. W. Ong, *Schwarz waveform relaxation with adaptive pipelining*, SIAM

Journal on Scientific Computing, 41 (2019), pp. A339–A364, https://doi.org/10.1137/17M115311X.

[22] B. C. Mandal, *Neumann–Neumann waveform relaxation algorithm in multiple subdomains for hyperbolic problems in 1D and 2D*, Numerical Methods for Partial Differential Equations, 33 (2017), pp. 514–530, https://onlinelibrary.wiley.com/doi/abs/10.1002/num.22112.

[23] R. K. Mohanty, *New unconditionally stable difference schemes for the solution of multi-dimensional telegraphic equations*, International Journal of Computer Mathematics, 86 (2009), pp. 2061–2071, https://doi.org/10.1080/00207160801965271.

[24] R. K. Mohanty, *An unconditionally stable difference scheme for the one-space-dimensional linear hyperbolic equation*, Applied Mathematics Letters, 17 (2009), pp. 101–105, https://www.sciencedirect.com/science/article/pii/S0893965904900195.

[25] A. Monge and P. Birken, *A Multirate Neumann–Neumann Waveform Relaxation Method for Heterogeneous Coupled Heat Equations*, SIAM Journal on Scientific Computing, 41 (2018), pp. S86–S105, https://doi.org/10.1137/18M1187878.

[26] B. Ong, S. High, and F. Kwok, *Pipeline Schwarz Waveform Relaxation*, in Domain Decomposition Methods in Science and Engineering XXII, Springer International Publishing, 2016, pp. 363–370, https://link.springer.com/book/10.1007/978-3-319-18827-0.

[27] B. W. Ong and B. C. Mandal, *Pipeline implementations of Neumann–Neumann and Dirichlet–Neumann waveform relaxation methods*, Numerical Algorithms, 78 (2018), pp. 1–20, https://link.springer.com/article/10.1007/s11075-017-0364-3.

[28] G. Smith, *Numerical Solution of Partial Differential Equations (Finite Difference Methods)*, vol. Third Edition of Oxford Applied Mathematics and Computing Science Series, Oxford University Press, 1985, https://global.oup.com/academic/product/numerical-solution-of-partial-differential-equations-9780198596509?cc=de&lang=en&.

[29] B. Song, Y.-L. Jiang, and X. Wang, *Analysis of two new Parareal algorithms based on the Dirichlet-Neumann/Neumann-Neumann waveform relaxation method for the heat equation*, Numerical Algorithms, 86 (2021), pp. 1685–1703, https://link.springer.com/article/10.1007/s11075-020-00949-y.

[30] C. Strohm and C. Tischendorf, *Coupled Electromagnetic Field and Electric Circuit Simulation: A Waveform Relaxation Benchmark*, in Modeling, Simulation and Optimization of Complex Processes HPSC 2018, Springer International Publishing, 2021, pp. 165–200, https://link.springer.com/chapter/10.1007/978-3-030-55240-4_9.

[31] I. Tsukerman, A. Konrad, G. Meunier, and J. Sabonnadiere, *Coupled field-circuit problems: trends and accomplishments*, IEEE Transactions on Magnetics, 29 (1993), pp. 1701–1704, https://ieeexplore.ieee.org/document/250733.